Assessment of the impacts of cloud chemistry on surface SO_2 and sulfate levels in typical regions of China

Jianyan Lu[1], Sunling Gong[1,5]*, Jian Zhang[1], Jianmin Chen[2,3,4], Lei Zhang[1], Chunhong Zhou[1]*

[1] State Key Laboratory of Severe Weather, Key Laboratory of Atmospheric Chemistry of CMA, Institute of Atmospheric Composition, Chinese Academy of Meteorological Sciences, Beijing 100081, China

[2] Shanghai Key Laboratory of Atmospheric Particle Pollution and Prevention (LAP3), Department of Environmental Science and Engineering, Fudan Tyndall Centre, Institute of Atmospheric Sciences, Fudan University, Shanghai, China

[3] Center for Excellence in Urban Atmospheric Environment, Institute of Urban Environment, Chinese Academy of Science, Xiamen, China

[4] Shanghai Institute of Eco-Chongming (SIEC), No.3663 Northern Zhongshan Road, Shanghai 200062, China

[5] National Observation and Research Station of Coastal Ecological Environments in Macao, Macao Environmental Research Institute, Macau University of Science and Technology, Macao SAR 999078, China

* Corresponding authors.

E-mail addresses: gongsl@cma.gov.cn (S. Gong), zhouch@cma.gov.cn (C. Zhou)

Abstract

A regional online chemical weather model WRF/CUACE (China Meteorological Administration Unified Atmospheric Chemistry Environment) is used to assess the contributions of cloud chemistry to the SO_2 and sulfate levels in typical regions of China. By comparing with several time series of in-situ cloud chemical observations on Mountain Tai in Shandong Province of China, the CUACE cloud chemistry scheme is found to reasonably reproduce the observed cloud consumption of H_2O_2, O_3 and SO_2 and the production of sulfate, and consequently is used in the regional assessment for a heavy pollution episode and monthly average of December 2016. During the cloudy period in the heavy pollution episode, the sulfate production was increased by 60-95% and SO_2 was reduced by over 80%. The cloud chemistry mainly affects the middle and lower troposphere below 5 km as well as within the

boundary layer, and contributes significantly to the SO_2 reduction and sulfate production in east-central China. Among the four typical regions in China, the Sichuan Basin (SCB) is mostly affected by the cloud chemistry, with the average of SO_2 abatement about 1.0-10.0 ppb and of sulfate increase about 10.0-70.0 μg/m^3, followed by Yangtze River Delta (YRD) and southeast of North China Plain (NCP), where SO_2 abatement is about 1.0-5.0 ppb and sulfate increase is about 10.0-30.0 μg/m^3. However, the cloud chemistry contributions to the Pearl River Delta (PRD) and northwest of NCP are not significant due to lighter pollution and less water vapor than other regions.

Keywords: SO_2, sulfate, cloud chemistry, WRF/CUACE

1. Introduction

Aerosols interact with radiation and clouds, directly or indirectly affecting the atmospheric radiation balance and precipitation, which in turn affects weather and climate (Twomey et al., 1984; Twomey, 1991; Charlson et al., 1992; Ramanathan et al., 2001; Pye et al., 2020). Moreover, large amounts of aerosols dispersed in the atmosphere can reduce visibility and deteriorate air quality (Molina, 2002), which is harmful to human health and ecosystem (Xie et al., 2019; Sielski et al., 2021).

In addition to direct emissions, aerosols are mostly produced secondarily through the oxidation of precursor gases, and one of the important processes is the transformation in clouds. Global cloud coverage of about 21% to 95% provides an adequate environment for cloud chemistry processes (Kotarba, 2020; Ravishankara, 1997). As about 90% of the clouds formed in the atmosphere evaporate without deposition or forming precipitation, large fractions of aerosols formed within clouds can then re-enter the atmosphere (Caffrey et al., 2001; Harris et al., 2013; Lelieveld and Heintzenberg, 1992). Globally, sulfate production from SO_2 oxidation accounts for about 80% of total sulfate, and more than half of it is produced in clouds (Hung et al., 2018; Faloona et al., 2010; Guo et al., 2012). Ge et al. (2021) found that cloud chemistry processes reduced the SO_2 concentrations by 0-50% in most of east-central China in all seasons. Li (2011) found that the average sulfate concentration in cloud water accounted for 53.8% of the total aerosol concentration at a mountain site. Li (2020) also found that cloud processes effectively reduced atmospheric O_3 and SO_2 concentrations by an average of 19.7% and 71.2%,

respectively, at Mount Tai.

Multiphase oxidation of SO_2 in aerosol particles in high humidity environment is one of the main causes of explosive growth of particulate matter in East Asia haze (Guo et al., 2014; Cheng et al., 2016; Song et al., 2019). From observations and laboratory works, four main pathways were identified for this kind of oxidation of SO_2, i.e. by H_2O_2, O_3, NO_2, and transition metal ions (TMIs) (Iibusuki and Takeuchi, 1987; Martin and Good, 1991; Alexander et al., 2009; Harris et al., 2013; Cheng et al., 2016; Wang et al., 2016; Wang et al., 2021). Additional pathways of organic peroxides (ROOH) (Yao et al., 2019; Wang et al., 2019; Ye et al., 2018; Dovrou et al., 2019), photolysis products of nitrate (pNO_3^-) (Gen et al., 2019b, a), and excited triplet states of photosensitizer molecules (T*) (Wang et al., 2020) have also been found recently to be important for multiphase oxidation of SO_2 during very heavy hazy days. Unfortunately, there are still many uncertainties and gaps to put all those pathways into model applications from observational and laboratory studies (Pye et al., 2020; Ravishankara, 1997; Liu et al., 2021). Several regional and global models have tried to include only O_3 and H_2O_2 in-cloud oxidant in cloud chemistry mechanisms (Park and Jacob, 2003; Tie, 2005; Von Salzen et al., 2000; Chapman et al., 2009; Leighton and Ivanova, 2008; Ivanova and Leighton, 2008), but only a few models can simulate the pathway of NO_2, TMIs of Fe or Mn ions (Chang et al., 1987; Binkowski and Roselle, 2003; Menut et al., 2013; Terrenoire et al., 2015; Ge et al., 2021).

There has been very serious air pollution in central-east China where four heavy pollution regions of North China Plain (NCP), Yangtze River Delta (YRD), Sichuan Basin (SCB) and Pearl River Delta (PRD) are located (Yao et al., 2021; Zhang et al., 2012). Although many global and regional models have contained sulfate formation mechanisms by cloud chemistry, few models have assessed its contribution, especially the lack of detailed assessment of regional cloud chemistry on sulfate and SO_2 in China. Some models have failed to reproduce SO_2 and sulfate observations, particularly underestimating sulfate and overestimating SO_2 over China (Buchard et al., 2014; Cheng et al., 2016; Hong et al., 2017a; Wei et al., 2019), which is mainly caused by the uncertainties in meteorological conditions (Sun et al., 2016) and emission inventories (Hong et al., 2017b; Sha et al., 2019b), as well as unclear and/or inaccurate physical and chemical mechanisms associated with air pollutants (He and Zhang, 2014; He et

al., 2015; Georgiou et al., 2018; Sha et al., 2019a). The inadequate inclusion or lack of cloud chemistry of SO_2 is one of the main causes (Ge et al., 2021). Therefore, it is very important and necessary to quantify the contribution of cloud chemistry in these regions and get a better understand of multi-dimensional pollution interactions, especially between the upper layer and the surface.

This study is intended to use an on-line coupled chemical weather platform of WRF/CUACE, to analyze and evaluate the SO_2 in-cloud oxidation process in the four polluted regions in China, with two objectives: (1) evaluating the cloud chemistry scheme in WRF/CUACE by the in-situ cloud chemistry observations at Mount Tai in summers of 2015 and 2018; and (2) quantifying the contributions of cloud chemistry to the SO_2 and sulfate changes in a typical winter pollution month of December 2016 with a very long lasting heavy pollution episode. It is aimed to establish a system to assess the relative contribution of cloud chemistry to SO_2 oxidation and sulfate productions vs. other clear-sky processes.

2. Model description and Methodology

2.1 Cloud chemistry in WRF/CUACE

WRF/CUACE is an on-line coupled chemical weather model under the WRF frame work with a comprehensive chemical module - CUACE, which is developed at CMA (China Meteorological Administration) with a sectional aerosol physics, gas chemistry, aerosol-cloud interactions and thermodynamic equilibrium (Zhou et al., 2012; Zhou et al., 2016; Gong et al., 2003; Gong and Zhang, 2008; Zhang et al., 2021), and treats seven types of aerosols, i.e. black carbon, organic carbon, sulfate, nitrate, ammonium, soil dust, and sea salt, and more than 60 gaseous species. The system can simulate the concentrations of PM_{10}, $PM_{2.5}$ and O_3 as well as visibility. A complete heterogeneous chemistry module has been built in CUACE for nine gas-to-particle heterogeneous reactions including SO_2 to sulfate (Zhou et al., 2021a; Zhang et al., 2021). The cloud chemistry mechanism in CUACE considers the pathways of multiphase oxidation of SO_2 by H_2O_2 and O_3 in both stratocumulus and convective clouds (Gong et al., 2003; Von Salzen et al., 2000). The transport and chemical effects of sulfur in convective clouds are calculated based on a convective cloud model by WRF. Within the cloudy part of a grid box, the first-order rate constant (in s^{-1}) of S(IV) oxidation is given by the following expression:

$$F = \left| \frac{1}{C_{S(IV)}} \frac{\mathrm{d}C_{S(IV)}}{dt} \right| = F_1 C_{O_3} + F_2 C_{H_2O_2} \quad (1)$$

where $C_{S(IV)}$ is the total concentration of S(IV) (gas phase plus dissolved), C_{O_3} is the total concentration of O_3, and $C_{H_2O_2}$ is the total concentration of hydrogen peroxide.

The effective rate constants F_1 and F_2 are given by the following expressions:

$$F_1 = R_{O_3} f_1 \quad (2)$$

$$F_2 = R_{H_2O_2} f_2 \quad (3)$$

The reaction rate constants of R_{O_3} and $R_{H_2O_2}$ refer to Maahs (Maahs, 1983) and Martin et al. (1984):

$$R_{O_3} = \left\{ 4.4\times10^{11} \exp(-4131/T) + 2.61\times10^{3} \exp(-966/T) \left[H^+\right]^{-1} \right\} (Ms)^{-1} \quad (4)$$

$$R_{H_2O_2} = 8\times10^{4} \exp\left[-3650(1/T - 1/298)\right] \left\{ 0.1 + \left[H^+\right] \right\}^{-1} (Ms)^{-1} \quad (5)$$

In Equations (2) and (3), the factors of f_1 and f_2 represent the partitioning of the substance between the aqueous and gas phases and are determined by the Henry's law coefficients.

$$f_1 = \gamma f_{SO_2} f_{O_3} K_S \overline{K}_{HO} \quad (6)$$

$$f_2 = \gamma f_{SO_2} f_{H_2O_2} \overline{K}_{HS} \overline{K}_{HP} \quad (7)$$

where γ is the dimensionless volume fraction of liquid water in the cloud. The parameters of f_{SO_2}, f_{O_3} and $f_{H_2O_2}$ are the proportions of individual substances in the gas phase, which are calculated from the dimensionless Henry's law constant and γ.

$$f_{SO_2} = \left(1 + \gamma \overline{K}_{HS} K_S\right)^{-1} \quad (8)$$

$$f_{O_3} = \left(1 + \gamma \overline{K}_{HO}\right)^{-1} \quad (9)$$

$$f_{H_2O_2} = \left(1 + \gamma \overline{K}_{HP}\right)^{-1} \quad (10)$$

with

$$K_S = \overline{K}_{HS}\left(1 + \frac{K_{1S}}{\left[H^+\right]} + \frac{K_{1S}K_{2S}}{\left[H^+\right]^2}\right) \quad (11)$$

The Henry's law constants used in (6) to (8) are listed in Table 1.

In order to consider the dependence of the oxidation rates on the pH, the H^+ concentration is calculated from ions balance.

$$\left[H^+\right] + \left[NH_4^+\right] = \left[OH^-\right] + 2\left[SO_4^{2-}\right] + 2\left[SO_3^{2-}\right] + \left[HSO_3^-\right] + \left[NO_3^-\right] + \left[HCO_3^-\right] \quad (12)$$

From Eqs. (1) ~ (12), CUACE can simulate the oxidation rates of SO_2 by H_2O_2 and O_3 mainly in the liquid and gaseous environment in both stratocumulus and convective clouds in three-dimensional way.

2.2 Assessment criteria

Three variables, RTCLD, DT, and RT, are defined to assess the impact of the cloud chemistry on SO_2 and sulfate. RTCLD refers to the concentration change ratio of substance i before and after the cloud chemical processes in a model run.

$$RTCLD(i) = 1 - \frac{BECLD(i)}{AFCLD(i)} \quad (13)$$

where BECLD and AFCLD denote the concentrations of component i before and after the cloud chemical processes, respectively, and i denotes the chemical component of SO_2, O_3, H_2O_2, and sulfate.

The DT indicates the difference in concentration of substance i with (CLD) and without (nCLD) cloud chemistry module activated.

$$DT(i) = CLD(i) - \mathrm{n}CLD(i) \tag{14}$$

and the RT represents the concentration ratio change of the substance i with and without cloud chemistry in separate model runs:

$$RT(i) = 1 - \frac{\mathrm{n}CLD(i)}{CLD(i)} \tag{15}$$

2.3 Methodology

2.3.1 Model Evaluation – Case 1

Mount Tai with an altitude of 1483 meter, located in central Shandong Province, is the highest point of the North China Plain. It is an ideal observation site for cloud chemistry observation (Li et al., 2017a; Li et al., 2020a; Li et al., 2020b). The observed concentrations of SO_2, O_3, H_2O_2 and sulfate in cloudy conditions from June 19 to July 30, 2015 and from June 20 to July 30, 2018 with time interval of 1 h are obtained to evaluate the cloud chemistry scheme in WRF/CUACE (Li et al., 2017a; Li et al., 2020a; Li et al., 2020b).

The WRF/CUACE is set up with two-level nesting domains for the evaluation with the Riguan Peak as the central point (Fig. 1a). The horizontal resolution of outer domain (O) is 9 km with a grid of 100×104, and of the inner domain (I) is 3 km with a grid of 88×94 (Fig. 1a). There are 32 vertical layers with the top pressure of 100 hPa.

2.3.2 Simulations of Regional Characteristics – Case 2

December 2016 was selected to assess the regional contribution of cloud chemistry to SO_2 and sulfate in CUACE when a typical heavy pollution episode occurred from Dec. 16 to 22, covering most part of east China with the highest hourly $PM_{2.5}$ concentration exceeding 1100 μg/m^3. The simulation

region is set up as shown in Figure 1b with two-level nesting domains. The outer domain (O) covers Central and East Asia with a horizontal resolution of 54 km and a grid of 139×112. The inner domain (I) covers most of China on the eastern side of the Qinghai-Tibet Plateau including NCP, YRD, PRD and SCB, with a horizontal resolution of 18 km and a grid of 157×166. The vertical layer number of the model is the same as that in the Case 1.

Since the cloud water is the reaction pool of cloud chemistry, whether the simulation of cloud water is reasonable or not is directly related to the effectiveness of cloud chemistry. Both the cloud water and rainwater from WRF are on-line coupled to the cloud chemistry module and the main physics configurations are listed in Table 2.

2.4 Meteorological, Pollution and Satellite Data

For both cases, the meteorological initial and boundary conditions for WRF/CUACE are from National Centers for Environmental Prediction (NCEP) FNL global reanalysis at a resolution of 1˚×1˚ with 6-h interval. The chemical lateral boundary conditions are from National Oceanic and Atmospheric Administration (NOAA) Meteorological Laboratory Regional Oxidant Model (NALROM) (Liu et al., 1996). The model is run in a restart way with a 5-day spin-up.

FY-2G cloud image data from CMA with an 1 h interval is used to evaluate the cloud in both cases. Routine meteorological observations in 3 h interval from 23 meteorological stations of CMA for 2 m temperature, 2 m relative humidity, and 10 m wind speed and the hourly pollutants data for 55 city sites from the China National Environmental Monitoring Centre are used to evaluate the meteorological fields and pollutants for December 2016. For a city with several observation sites, an averaged value is used to presently the city.

The MEIC (Multi-resolution Emission Inventory for China) inventory, at a resolution of 0.25˚, is used as the anthropogenic emissions with the species of SO_2, nitrogen oxides NO_x, carbon monoxide (CO), ammonia (NH_3), black carbon (BC), organic carbon (OC), non-methane volatile organic compounds (NMVOCs), $PM_{2.5}$ and PM_{10} from industry, transportation, residential, and agriculture (Li et

al., 2017b; Zheng et al., 2018). The emission base years of 2015 and 2017 are used for Case-1 and Case-2, respectively.

3. Results and Discussions

3.1 Evaluation of the cloud chemistry mechanism

In order to evaluate the cloud chemistry mechanism in WRF/CUACE, the simulation results are compared with the observations at Mount Tai. By analyzing the satellite cloud images in and around Mount Tai and matching with the available observed data, two time periods with clouds from June 19 to July 30, 2015 and June 20 to July 30, 2018 were selected for the comparisons, defined as "cloud process-1" (CP-1) and "cloud process-2" (CP-2), respectively. The simulated results for chemical species are illustrated in scatter plots (Fig. 2), which reveals that the simulated concentrations of SO_2, sulfate, O_3, and H_2O_2 are all within a factor of two of the observations when cloud chemistry occurs, indicating reasonable agreement between simulations and observations for both CP-1 and CP-2 cases. The sulfate underestimates are clear in both CP-1 and CP-2 cases, which was reported by other modeling results before as well (Tuccella et al., 2012; Huang et al., 2019; Ge et al., 2022).

The statistics of correlation coefficients (R), relative average deviation (RAD), and normalized mean deviation (NMB) between hourly simulated and observed SO_2, O_3, H_2O_2 and sulfate are shown in Table 3. Among them, the simulated and observed averages of SO_2 are very close in both CP-1 and CP-2, with a RAD about -3.4% and -6.1%. For other species, the RAD is in the range of 8.7-55.0%. The Rs for the four species are 0.34, 0.33 and 0.78 and 0.32 for CP-1, and 0.47, 0.40, 0.06 and 0.54 for CP-2, respectively. Although the R, RAD, and NMB of H_2O_2 in CP-2 is only 0.06, 18.0%, and -19.6%, the simulated mean value of H_2O_2 is closer to the observed mean value than that in CP-1 (RAD = 22.4%, NMB = -36.6%). For sulfate, the simulated Rs are 0.32 and 0.54 in CP-1 and CP-2, respectively, but the model underestimates sulfate concentrations with NMB of -71.0% and -59.4% in CP-1 and CP-2. Some reasons might contribute to the underestimations. Firstly, the latitude of the observed site at Mount Tai is 1483 meters which can be in the boundary layer during the daytime and in the free atmosphere during the nighttime in summer (Zhu et al., 2018). Therefore, the diurnal variation of the boundary layer affects

the three-dimensional concentration distribution of oxidants and aerosols (Peng et al., 2021), and influences the development of cloud formation. Secondly, there are bias from the model due to the difficulties to represent the complex topography of Mount Tai and the cloud physics. Thirdly, the cloud chemistry in CUACE lacks the pathway for TMI-catalyzed oxidation and NO_2-catalyzed oxidation as well as some other newly discovered oxidation mechanisms which can lead to the bias in SO_2 and sulfate. Fourthly, typical measurement systems for ambient aerosols easily misinterpret organosulfur (mainly in the presence of hydroxy-methane sulfonate (HMS)) as inorganic sulfate, thus leading to a positive observational bias, e.g., 20% mean bias during winter haze in Beijing (Moch et al., 2018; Song et al., 2019).

Another interesting point simulated correctly by the model was the increasing trend of H_2O_2 and the decreasing trend of SO_2 from 2015 to 2018. The observed and simulated mean values of H_2O_2 were changed from 26.5 and 16.8 μM in CP-1 in 2015 to 46.9 and 32.4 μM in CP-2 in 2018, respectively. For SO_2, the observed and simulated mean values were reduced from 2.2 and 2.3 $\mu g/m^3$ in CP-1 in 2015 to 0.6 and 0.6 $\mu g/m^3$ in CP-2 in 2018, respectively in Table 3. Both the observations and simulations clearly showed the increasing trend of H_2O_2 and the decreasing trend of SO_2 from 2015 to 2018. This conclusion is consistent with the trends of other observational studies (Ren et al., 2009; Shen et al., 2012; Li et al., 2020a; Ye et al., 2021). The decreasing SO_2 and increasing H_2O_2 and O_3 have been tightly attributed to the national SO_2 and particulate emission control measures since 2013 (Fan et al., 2010; Lu et al., 2020).

Figure 4 shows the RTCLD of SO_2 and simulated liquid water contents at 2:00 and 8:00 LST on both June 24 and June 25 in CP-1 at Mount Tai. The column cloud and the liquid water contents which are consistent with the cloud images indicate that there is cloud with sufficient water vapor in and around the vicinity of Mount Tai (Fig. 3). The SO_2 consumption rate (RTCLD(SO_2)) distribution is consistent with the liquid water distribution at all four times (Fig. 4). The SO_2 depletion rate is above 80% at Mount Tai which is compatible to the observation (Li, 2020). All of these indicate that the model can capture the SO_2 consumption in the cloudy environment.

In summary, the simulated SO_2, H_2O_2, O_3 and sulfate concentrations are comparable to the

observations. WRF/CUACE is also able to simulate the decreasing trend of SO_2 and the increasing trends of O_3 and H_2O_2 with year. Therefore, the cloud chemistry mechanism in WRF/CUACE is relatively reasonable to reproduce the cloud chemistry for SO_2, sulfate and the important oxidants of H_2O_2 and O_3.

3.2 Assessment of the impacts of cloud chemistry on regional SO_2 and sulfate

This session will further assess the contribution of cloud chemistry for the four main pollution regions of NCP, YRD, PRD, and SCB (Fig. 1b) in China for the whole December of 2016 (hereinafter referred to as DEC) and a heavy pollution episode (hereinafter referred to as HPE) occurred during month (Dec. 16-22) as selected for Case 2. The regional impacts of cloud chemical processes on surface SO_2 and sulfate are analyzed for DEC and for HPE. The heavy pollution episode (HPE) is investigated with respect to the developing stage HPE-1 (Dec. 16-18, 2016), the maturity stage HPE-2 (Dec. 19-21, 2016) and to the dissipation stage HPE-3 (Dec. 22, 2016) for the four pollution regions.

3.2.1 Meteorological evaluation

As the driving force for air pollution and cloud chemistry, the meteorology elements of 2 m temperature (T2), 2 m relative humidity (RH2) and 10 m wind speed (WS10) in DEC and HPE are compared between simulated and observed results in Table 4. The temperature correlation is the best in DEC, followed by humidity and then wind speed, which is consistent with previous findings (Zhou et al., 2012; Wang et al., 2015; Gao et al., 2016). The RMSE of wind speeds all ranges from 1.03 to 1.50 m/s, falling within the criteria (less than 2 m/s) to define “good” model performance in stagnant weather (Emery et al., 2001). The RMSE of wind speed and the wind speed for HPE is smaller than that of DEC, which indicates that the model can relatively reasonably capture the static condition.

Figure 5 shows the satellite cloud images, the column cloud and the liquid water content simulated for the maturity and dissipation stages (Dec. 19-22) of the HPE. The satellite image shows that the cloud coverage region is mainly in the southwest of China besides SCB on the 19th, covering most of eastern China including NCP, YRD, PRD and SCB on the 20th and the 21st, and then moving eastward outside of

China on the 22nd (Fig. 5 a1-d1). The cloud distribution fits well with the satellite images (Fig. 5 a2-d2). The column liquid water distribution also moves from west to east as the episode developed (Fig. 5 a3-d3), which is located more southern part of eastern China than that of the clouds. In SCB and YRD, the liquid water content is more abundant, reaching over 100.0 g/m^2, than that in PRD, only up to 10.0 g/m^2. NCP has the least liquid water content among the four regions, especially in Beijing and northwestern part of Hebei Province ranging 0.001-0.01 g/m^2, mostly due to the dry environment and partly due to the overestimated temperature and underestimated humidity in the model. Above all, CUACE not only effectively simulates pollution but also provides a relatively reasonable meteorological background basis for cloud chemistry in the heavy pollution period.

3.2.2 Chemical evaluation

Figure 6 shows the mean SO_2 and sulfate concentrations simulated for DEC and HPE-2. The high and low centers of monthly mean SO_2 and sulfate concentrations by CUACE in December 2016 are coincided with the annual observed average by Gao et al. (2021) in the SCB and NCP. The sulfate concentrations are low on a monthly basis and high at the pollution maturity stage compared to the averaged observations of several pollution episodes studied by Wang et al. (2022) in December 2016 for NCP. The simulated mean sulfate concentration distribution in Figure 6b is comparable to that by Wang et al. (2021) and Wang et al. (2022) in December 2016, both displaying an increase from northwest to southeast almost in the same magnitude in NCP. For SCB, sulfate concentrations are compatible to the observed in winter in 2015 by Kong et al. (2020).

The simulated hourly $PM_{2.5}$, O_3 and SO_2 concentrations in four regions are also compared with the observations (Table 5). Most of the simulations are within a factor of two of the observations (figure omitted), and the mean values of the three pollutants in the four regions are close to the observations for DEC and HPE, indicating that the model captures the variability of $PM_{2.5}$, O_3 and SO_2 concentrations for both DEC and HPE. During HPE, the differences of mean values ranged from -7.6 to 10.4 μg/m^3 for SO_2, from -22 to 23.3 μg/m^3 for O_3, and from -156.5 to 48.8 μg/m^3 for $PM_{2.5}$. During DEC, the differences of mean values from -21.5 to -1.2 μg/m^3 for SO_2, from 1.1 to 7.7 μg/m^3 for O_3, and from -71.3 to 1.3 μg/m^3 for $PM_{2.5}$. During HPE, the Rs are from 0.32 to 0.61 for SO_2, from 0.20 to 0.84 for O_3, and from 0.27 to

0.84 for $PM_{2.5}$. During DEC, the Rs are from 0.19 to 0.48 for SO_2, from 0.47 to 0.80 for O_3, and from 0.28 to 0.73 for $PM_{2.5}$. During HPE, the NMBs are from -49.8 to 46.3 for SO_2, from -54.0 to 123.1 for O_3, and from -48.2 to 51.0 for $PM_{2.5}$. During DEC, the NMBs are from -47.4 to 11.9 for SO_2, from -45.5 to 97.4 for O_3, and from -35.7 to 51.5 for $PM_{2.5}$. The simulation in PRD, YRD and NCP is relatively better than that in the SCB, where the complex terrain poses great challenges to meteorological field simulations.

The ability of CUACE to simulate SO_2, O_3 and sulfate concentrations has also been evaluated in many previous research applications (Ke et al., 2020; Zhou et al., 2021b; Zhang et al., 2021) where Ke et al. (2020) reported that the correlation between CUACE modeled and observed $PM_{2.5}$ was 0.41-0.85 in NCP and 0.64-0.74 in YRD. The ability of other atmospheric models in China has the same performance such as NACRMS which has a correlation of about 0.68 for $PM_{2.5}$ in NCP during haze period (Wang et al., 2014).

3.2.3 Assessment of regional contributions

In order to assess the regional contributions, the average monthly impact of cloud chemistry on surface SO_2 and sulfate demoted by DT(SO_2) and DT (sulfate) for DEC is investigated (Fig. 7). It is found that the SO_2 declination for DEC is concentrated mostly in the central-eastern part of China, by an average of 0.1-1.0 ppb in most regions by cloud chemistry. SO_2 concentrations are reduced by 0.5-3.0 ppb in most part of NCP, YRD, PRD and SCB regions. Among them, there is a relatively strong center by declining 3.0-10.0 ppb in SCB. Ge et al. (2021) have evaluated the effects of in-cloud aqueous-phase chemistry on SO_2 oxidation by the Community Earth System Model version 2 (CESM2). They found that the results incorporating detailed cloud aqueous-phase chemistry greatly reduced the SO_2 overestimation, i.e., by 0.1-10.0 ppb in China and more than 10.0 ppb in some regions in winter, which is consistent with the results demonstrated in Figure 7, where SO_2 concentrations are depleted by 0.1-10 ppb in China. Correspondingly, sulfate growth is mainly centered in SCB, with the increased maximum up to 20.0-50.0 μg/m^3. Sulfate concentrations are increased by 10.0-20.0 μg/m^3 in most part of NCP, YRD and PRD, and 5-10.0 μg/m^3 in others.

In addition to the average monthly impact of cloud chemistry, Figure 8 shows the DT(SO_2) and

DT(sulfate) for the high pollution episode: HPE-2. It is found that the SO_2 concentration decreases most significantly in SCB, with 1.0-3.0 ppb in most region, up to 3.0-10.0 ppb in the central region. In YRD, PRD and NCP, the reduction reaches 1.0-3.0 ppb in most part while the smallest decrease is below 1.0 ppb in the northern part of NCP. Meanwhile, in terms of regional distribution, the regions of increasing sulfate and decreasing SO_2 concentrations are correlated, but not identical. Sulfate production is mainly focused in SCB, with the increasing maximum up to 20.0-50.0 μg/m^3, while the production is by 10.0-20.0 μg/m^3 in most part of NCP, YRD and PRD and by 5.0-10.0 μg/m^3 in other regions. In Figure 7b and Figure 8b, the increasing rates for monthly mean sulfate concentrations are about 60% to 70% in NCP. The heaviest and longest duration pollution episode that had a lot of clouds and high liquid water content (Fig. 5) on December 19-21, 2016, was very favorable for the occurrence of in-cloud oxidation processes. Sulfate formation rates by H_2O_2 oxidation under winter haze conditions range from 10 to 1000 μg/m^3/s, which is close to the range of 10 to 100 μg/m^3/s obtained by Wang et al. (2022) in several pollution episodes in December 2016, indicating that the in-cloud oxidation in this study is relatively reasonable.

Exploring details into the HPE, four time periods, 14:00 and 21:00 on the 20th, 17:00 on 21st of the HPE-2, and 12:00 on the 22nd of the HPE-3, are used to specifically analyze the contribution of cloud chemistry. It is found that the cloud chemistry influence is mainly on SCB and YRD at 14:00 and 21:00 LST on Dec. 20 for HPE-2. The observed $PM_{2.5}$ concentrations are very high, up to 350 μg/m^3 at 14:00 on the 20th and 236 μg/m^3 at 21:00 on the 20th in Chengdu of SCB, up to 76 μg/m^3 at 14:00 on the 20th and 77 μg/m^3 at 21:00 on the 20th in Hangzhou of YRD, partially supporting the cloud production of sulfate production at these specific times. Correspondingly, Figure 9 shows that sulfate increases by cloud chemistry during these time periods are 10-20 μg/m^3 and 20-30 μg/m^3 14:00 and 21:00 on 20th at Chengdu, 20-60 μg/m^3 and 30-60 μg/m^3 at Hangzhou.

Above all, the contribution of cloud chemistry to surface sulfate during the HPE is the highest in the SCB, followed by the NCP, YRD and PRD, with mostly concentration increases ranging 20.0-100.0 μg/m^3, 10.0-60.0 μg/m^3, and 10.0-40.0 μg/m^3, 10.0-40.0 μg/m^3, respectively, and less than 10.0 μg/m^3 in Beijing, Tianjin and the northwestern part of Hebei Province (Fig. 9). Of particular note is the North

China region, where the contribution of cloud chemistry is not significant on a monthly average but is very significant and exceeds that for YRD region at certain moments during HPE. This also provides an explanation for the explosive increase in particulate matter concentrations during HPE in this region.

Further analysis of the simulation characteristics with and without cloud chemistry on all the regions during the HPE-2 stage (Fig. 10) and the DEC (Fig. 11), is carried out. Compared with nCLD, R of SO_2 in CLD increases by 0.06, 0.15, and 0.01 in YRD, SCB, and NCP, respectively, and the overestimation in NCP and PRD has been corrected during HPE-2. R also increases by 0.10, 0.03 and 0.05 in YRD, SCB and NCP for the DEC, respectively. It is obvious that the model simulates SO_2 concentrations better at NCP during HPE-2 than for DEC with cloud chemistry.

For $PM_{2.5}$, the statistical results of the simulated mean, R and NMB in CLD and nCLD in the four polluted regions do not differ significantly between HPE-2 and DEC, but there is a significant improvement in the underestimate of sulfate in NCP and SCB. Under cloud chemistry, the deviation in the NCP is reduced from -45.7% to -35.7% for DEC and from -52.6% to -48.2% for HPE-2. The deviation in SCB is also improved from -44.2% to -29.1% for DEC and from -46.5% to -32.9% for HPE-2. A significant reduction in the model's $PM_{2.5}$ concentration simulation bias after considering cloud chemistry, and an improvement in the underestimation at NCP and SCB has been achieved.

Moreover, the statistical results of all stations (SUM in Fig. 12) show that after considering cloud chemical simulation (CLD), the NMB of SO_2 is decreased from 39.3% to 13.8% and the NMB of $PM_{2.5}$ from -40.8% to -31.6% during the HPE-2 after the addition of cloud chemistry simulation, reducing the simulation bias of both SO_2 and $PM_{2.5}$. This indicates that the addition of cloud chemistry to the model improves the model for SO_2 and sulfate simulations. The improvement of sulfate simulation in the presence of clouds also contributes to the improvement of the simulation accuracy of $PM_{2.5}$ mentioned above.

In summary, comparing the contribution of cloud chemistry in DEC with HPE-2, it is found that the cloud chemistry in heavy pollution weather for SO_2 depletion and sulfate increase is mainly concentrated in the central-eastern part of China, and the four major pollution regions are also obvious.

However, SO_2 consumption and sulfate increase are not consistent, which is not only influenced by the local SO_2 concentration, but also by the cloud amount. Therefore, for SCB, where there is less polluted and has much more clouds than that in NCP, the impact of cloud chemistry on sulfate and its precursor SO_2 is always the most significant, for both HPE and DEC.

3.3 Site evaluation of cloud chemistry

The statistical metrics of SO_2 and $PM_{2.5}$ hourly concentrations in 55 representative cities with and without cloud chemistry in the model were analyzed. The results indicate that most of the sites are improved with cloud chemistry in the SO_2 concentration simulation and 42 of the 55 cities are with the increasing R. In the $PM_{2.5}$ simulation, the correlations also are improved in some cities after the presence of cloud chemistry.

Representative sites of Beijing, Nanjing, Guangzhou and Chengdu at NCP, YRD, PRD and SCB are selected to quantify the impact of cloud chemistry during the HPE. The net depletion ratio of SO_2 column concentration ($RT(SO_2)$) during cloud chemistry is shown in Figure 13. It is found that SO_2 column concentration reduction maintained mostly a high value of over 60%, even to 80% sometimes, in Chengdu during HPE-2. In Nanjing, the SO_2 level was reduced by about 20-50% from 17^{th} to 19^{th} and up to 80% from 20^{th} to 21^{st} when the episode matured there. The changes of SO_2 in these two cities are consistent with the changes in cloud and liquid cloud water content distributions during the HPE-2 in Figure 3. The SO_2 reduction in Beijing and Guangzhou was consistently maintained at around 40% during the period from 17^{th} to 21^{st}. The lower oxidative transformation was related to the lower liquid water content in Beijing, while in Guangzhou it was attributed to the combination of low pollution levels and low cloud water content. Figure 3 showed that Chengdu maintained abundant water vapor conditions from 17^{th} to 21^{st}, and so did Nanjing from 20^{th} to 21^{st}. However, the ambient water vapor content was quite low in Guangzhou and Beijing throughout the process and the SO_2 oxidation was much lower than that of Chengdu and Nanjing. In conclusion, the cloud chemistry process can lead to SO_2 column concentration consumption share of more than 60% when cloud water content is abundant, which is also consistent with the observations of Mount Tai by Li (2020).

The impact of cloud chemistry (RT) on surface SO_2 and sulfate in four sites is also shown in Figure 13. The overall trend shows that the peak and valley timing of surface SO_2 consumption and sulfate increase are coincident. The cloud chemical processes of the surface SO_2 oxidation vary greatly between cities in different regions (Fig. 14a). In HPE-2, the percentage of surface SO_2 consumption reached more than 90% in Chengdu and Nanjing, while it was below 30% in Beijing and Guangzhou, and did not reach 40% until the 22nd. Although the percentage of surface SO_2 consumption varies greatly, the increase in the percentage of sulfate does not vary much between cities. In HPE-2, the increase in surface sulfate in the four cities ranged from 60-95% (Fig. 14b), which is consistent with the sulfate increase rates summarized by Turnock et al. (2019).

Figure 15 is the variation of vertical profiles of sulfate increase by the cloud chemistry at the four times at 12:00 LST on Dec. 20 for HPE-2, at 04:00 LST on Dec. 21 for HPE-2, at 04:00 and 12:00 LST on Dec. 22 for HPE-3 in Beijing, Nanjing, Chengdu and Guangzhou. It shows that the sulfate produced by the cloud chemistry during this pollution process is concentrated mostly below 5 km in the troposphere, especially under 2 km. Again, less sulfate has been produced in Beijing in vertical than that of others by the cloud chemistry.

4. Summary and conclusions

The cloud chemistry mechanism in WRF/CUACE has been assessed by using the in-situ cloud chemistry observations of SO_2, O_3, and H_2O_2 from Mount Tai in June-July of 2015 and 2018. The results show that the mechanism has well captured the cloud processes for the oxidation of SO_2, reducing SO_2 by more than 80% during the cloudy phase, which is in good agreement with the observations.

The cloud chemistry contributions to the changes of SO_2 and sulfate concentrations in NCP, YRD, PRD and SCB regions are assessed by WRF/CUACE. During heavy pollution (HPE-2), the four regions are significantly affected by cloud chemistry, with SCB being the most obvious. The surface SO_2 reduction in SCB ranges 1.0-3.0 ppb and reaches 3.0-10.0 ppb in the high value areas, and surface sulfate concentration is increased by 10.0-30.0 μg/m^3 on average, with a maximum of more than 20.0-70.0 μg/m^3. Most areas in NCP, YRD and PRD have an average SO_2 reduction of 0.5-3.0 ppb and sulfate

increase of 5.0-30.0 μg/m^3. Although the monthly average impact of cloud chemistry is much weaker in the NCP due to less water vapor in December, the contribution in the southern part of NCP during heavy pollution time is still significant and cannot be ignored. In PRD, the contribution of cloud chemistry is weaker than other regions due to lighter pollution, although there are lots of clouds with abounded liquid water there. In addition, the cloud chemistry increases surface sulfate concentration by 60-95% and reduces surface SO_2 concentration by more than 80% in Beijing, Nanjing, Chengdu and Guangzhou during HPE-2. Above all, the average contribution of cloud chemistry during HPE-2 is significantly greater than that for DEC. Vertically, the cloud chemistry influence is mainly in the middle and lower troposphere below 2 km for four representative cities in HPE-2. Generally, the cloud chemistry can improve the model performance by reducing the overestimates of SO_2 and underestimates of sulfate.

In the future, more mechanisms should be added to improve the cloud chemistry mechanism in CUACE, and more accurate to simulate SO_2 and sulfate and other aerosol components such as nitrate, ammonium, carbonate, and organic aerosols.

Code/data availability

All source code and data can be accessed by contacting the corresponding authors Sunling Gong (gongsl@cma.gov.cn).

Authors contribution

CZ and SG put forward the ideas and formulated overarching research goals. JL carried them out and wrote the manuscript with suggestions from all authors. LZ and JZ participated in the scientific interpretation and discussion. JC assisted with data acquisition and processing. All authors contributed to the discussion and improvement of the manuscript.

Competing interests

The authors declare that they have no conflict of interest.

Financial support

This research has been supported by the National Key Project of the Ministry of Science and Technology of China (2022YFC3701205); CMA Innovation Development Project (CXFZ2021J023).

References

Alexander, B., Park, R. J., Jacob, D. J., and Gong, S.: Transition metal-catalyzed oxidation of atmospheric sulfur: Global implications for the sulfur budget, Journal of Geophysical Research, 114, D02309, https://doi.org/10.1029/2008jd010486, 2009.

Binkowski, F. S. and Roselle, S. J.: Models-3 Community Multiscale Air Quality (CMAQ) model aerosol component 1. Model description, Journal of Geophysical Research: Atmospheres, 108, 4183, https://doi.org/10.1029/2001jd001409, 2003.

Buchard, V., da Silva, A. M., Colarco, P., Krotkov, N., Dickerson, R. R., Stehr, J. W., Mount, G., Spinei, E., Arkinson, H. L., and He, H.: Evaluation of GEOS-5 sulfur dioxide simulations during the Frostburg, MD 2010 field campaign, Atmospheric Chemistry and Physics, 14, 1929-1941, https://doi.org/10.5194/acp-14-1929-2014, 2014.

Caffrey, P., Hoppel, W., Frick, G., Pasternack, L., Fitzgerald, J., Hegg, D., Gao, S., Leaitch, R., Shantz, N., Albrechcinski, T., and Ambrusko, J.: In-cloud oxidation of SO2by O3 and H2O2: Cloud chamber measurements and modeling of particle growth, Journal of Geophysical Research: Atmospheres, 106, 27587-27601, https://doi.org/10.1029/2000jd900844, 2001.

Chang, J. S., Brost, R. A., Isaksen, I. S. A., Madronich, S., Middleton, P., Stockwell, W. R., and Walcek, C. J.: A three-dimensional eulerian acid deposition model physical concepts and formulation, journal of geophysical research, 92, 14681-14700, https://doi.org/10.1029/jd092id12p14681, 1987.

Chapman, E. G., Gustafson, W. I., Easter, R. C., Barnard, J. C., and Fast, J. D.: Coupling aerosol-cloud-radiative processes in the WRF-Chem model: Investigating the radiative impact of elevated point sources, Atmos. Chem. Phys., 9, 945-964, https://doi.org/10.5194/acp-9-945-2009, 2009.

Charlson, R., J., Schwartz, and S., E.: Climate forcing by anthropogenic aerosols, Science, 255, 423-423, https://doi.org/10.1126/science.255.5043.423, 1992.

Cheng, Y., Zheng, G., Wei, C., Mu, Q., Zheng, B., Wang, Z., Gao, M., Zhang, Q., He, K., and Carmichael, G.: Reactive nitrogen chemistry in aerosol water as asource of sulfate during haze events in China, Science Advances, 2, e1601530, https://doi.org/10.1126/sciadv.1601530, 2016.

Dovrou, E., Rivera-Rios, J. C., Bates, K. H., and Keutsch, F. N.: Sulfate Formation via Cloud Processing from Isoprene Hydroxyl Hydroperoxides (ISOPOOH), Environ Sci Technol, 53, 12476-12484, https://doi.org/10.1021/acs.est.9b04645, 2019.

Emery, C., Tai, E., and Yarwood, G.: Enhanced meteorological modeling and performance evaluation for two Texas ozone episodes, Corpus ID 127579774, 2001.

Faloona, I., Conley, S. A., Blomquist, B., Clarke, A. D., Kapustin, V., Howell, S., Lenschow, D. H., and Bandy, A. R.: Sulfur dioxide in the tropical marine boundary layer: dry deposition and heterogeneous oxidation observed during the Pacific Atmospheric Sulfur Experiment, Journal of Atmospheric Chemistry, 63, 13-32, https://doi.org/10.1007/s10874-010-9155-0, 2010.

Fan, D., Ye. Y., and Wang, W.: Air Pollution Control and Public Health:Evidence from “Air Pollution Prevention and Control Action Plan” in China, Statistical Research, 38, 60-74, https://doi.org/10.19343/j.cnki.11-1302/c.2021.09.005, 2010.

Gao, M., Carmichael, G. R., Wang, Y., Ji, D., Liu, Z., and Wang, Z.: Improving simulations of sulfate aerosols during winter haze over Northern China: the impacts of heterogeneous oxidation by NO2, Frontiers of Environmental Science & Engineering, 10, 11, https://doi.org/10.1007/s11783-016-0878-2, 2016.

Ge, W., Liu, J., Xiang, S., Zhou, Y., Zhou, J., Hu, X., Ma, J., Wang, X., Wan, Y., Hu, J., Zhang, Z., Wang, X., and Tao, S.: Improvement and uncertainties of global simulation of sulfate concentration and radiative forcing in CESM2, Journal of Geophysical Research: Atmospheres, 127, e2022JD037623, https://doi.org/10.1029/2022JD037623, 2022.

Ge, W., Liu, J., Yi, K., Xu, J., Zhang, Y., Hu, X., Ma, J., Wang, X., Wan, Y., Hu, J., Zhang, Z., Wang, X.,

and Tao, S.: Influence of atmospheric in-cloud aqueous-phase chemistry on global simulation of SO2 in CESM2, Atmospheric Chemistry and Physics, 21, 16093-16120, https://doi.org/10.5194/acp-2021-406, 2021.

Gen, M., Zhang, R., Huang, D. D., Li, Y., and Chan, C. K.: Heterogeneous Oxidation of SO(2) in Sulfate Production during Nitrate Photolysis at 300 nm: Effect of pH, Relative Humidity, Irradiation Intensity, and the Presence of Organic Compounds, Environ Sci Technol, 53, 8757-8766, https://doi.org/10.1021/acs.est.9b01623, 2019a.

Gen, M., Zhang, R., Huang, D. D., Li, Y., and Chan, C. K.: Heterogeneous SO2 Oxidation in Sulfate Formation by Photolysis of Particulate Nitrate, Environmental Science & Technology Letters, 6, 86-91, https://doi.org/10.1021/acs.estlett.8b00681, 2019b.

Georgiou, G. K., Christoudias, T., Proestos, Y., Kushta, J., Hadjinicolaou, P., and Lelieveld, J.: Air quality modelling in the summer over the eastern Mediterranean using WRF-Chem: chemistry and aerosol mechanism intercomparison, Atmospheric Chemistry and Physics, 18, 1555-1571, https://doi.org/10.5194/acp-18-1555-2018, 2018.

Gong, S. and Zhang, X.: CUACE/Dust–an integrated system of observation and modeling systems for operational dust forecasting in Asia, Atmospheric Chemistry and Physics, 8, 2333-2340, https://doi.org/10.5194/acp-8-2333-2008, 2008.

Gong, S. L., Barrie, L. A., Blanchet, J. P., von Salzen, K., Lohmann, U., Lesins, G., Spacek, L., Zhang, L. M., Girard, E., Lin, H., Leaitch, R., Leighton, H., Chylek, P., and Huang, P.: Canadian Aerosol Module: A size-segregated simulation of atmospheric aerosol processes for climate and air quality models 1. Module development, Journal of Geophysical Research, 108, 4007, https://doi.org/10.1029/2001jd002002, 2003.

Guo, J., Wang, Y., Shen, X., Wang, Z., Lee, T., Wang, X., Li, P., Sun, M., Jeffrey, L., Collett, J., Wang, W., and Wang, T.: Characterization of cloud water chemistry at Mount Tai, China: Seasonal variation, anthropogenic impact, and cloud processing, Atmospheric Environment, 60, 467-476,

10.1016/j.atmosenv.2012.07.016, 2012.

Guo, S., Hu, M., Zamora, M. L., Peng, J., Shang, D., Zheng, J., Du, Z., Wu, Z., Shao, M., Zeng, L., Molina, M. J., and Zhang, R.: Elucidating severe urban haze formation in China, Proc Natl Acad Sci U S A, 111, 17373-17378, https://doi.org/10.1073/pnas.1419604111, 2014.

Harris, E., Sinha, B., van Pinxteren, D., Tilgner, A., Fomba, K. W., Schneider, J., Roth, A., Gnauk, T., Fahlbusch, B., Mertes, S., Lee, T., Collett, J., Foley, S., Borrmann, S., Hoppe, P., and Herrmann, H.: Enhanced role of transition metal ion catalysis during in-cloud oxidation of SO2, Science, 340, 727-730, https://doi.org/10.1126/science.1230911, 2013.

He, J. and Zhang, Y.: Improvement and further development in CESM/CAM5: gas-phase chemistry and inorganic aerosol treatments, Atmospheric Chemistry and Physics, 14, 9171-9200, https://doi.org/10.5194/acp-14-9171-2014, 2014.

He, J., Zhang, Y., Glotfelty, T., He, R., Bennartz, R., Rausch, J., and Sartelet, K.: Decadal simulation and comprehensive evaluation of CESM/CAM5.1 with advanced chemistry, aerosol microphysics, and aerosol-cloud interactions, Journal of Advances in Modeling Earth Systems, 7, 110-141, https://doi.org/10.1002/2014ms000360, 2015.

Hong, C., Zhang, Q., Zhang, Y., Tang, Y., Tong, D., and He, K.: Multi-year downscaling application of two-way coupled WRF v3.4 and CMAQ v5.0.2 over east Asia for regional climate and air quality modeling: model evaluation and aerosol direct effects, Geoscientific Model Development, 10, 2447-2470, https://doi.org/10.5194/gmd-10-2447-2017, 2017a.

Hong, C., Zhang, Q., He, K., Guan, D., Li, M., Liu, F., and Zheng, B.: Variations of China's emission estimates: response to uncertainties in energy statistics, Atmospheric Chemistry and Physics, 17, 1227-1239, https://doi.org/10.5194/acp-17-1227-2017, 2017b.

Huang, L., An, J., Koo, B., Yarwood, G., Yan, R., Wang, Y., Huang, C., and Li, L.: Sulfate formation during heavy winter haze events and the potential contribution from heterogeneous SO2 +NO2 reactions

in the Yangtze River Delta region, China, Atmospheric Chemistry and Physics, 19, 14311-14328, https://doi.org/10.5194/acp-19-14311-2019, 2019.

Hung, H. M., Hsu, M. N., and Hoffmann, M. R.: Quantification of SO2 Oxidation on Interfacial Surfaces of Acidic Micro-Droplets: Implication for Ambient Sulfate Formation, Environ Sci Technol, 52, 9079-9086, https://doi.org/10.1021/acs.est.8b01391, 2018.

IIbusuki, T. and Takeuchi, K.: Sulfur dioxide oxidation by oxygen catalyzed by mixtures of manganese(II) and iron(III) in aqueous solutions at environmental reaction conditions, Atmospheric Environment, 21, 1555-1560, https://doi.org/10.1016/0004-6981(87)90317-9, 1987.

Ivanova, I. T. and Leighton, H. G.: Aerosol–Cloud Interactions in a Mesoscale Model. Part II: Sensitivity to Aqueous-Phase Chemistry, Journal of the Atmospheric Sciences, 65, 309-330, https://doi.org/10.1175/2007jas2276.1, 2008.

Ke, H., Gong, S., He, J., Zhou, C., Zhang, L., and Zhou, Y.: Assessment of Open Biomass Burning Impacts on Surface PM2.5 Concentration, Chinese Academy of Meteorological Sciences, 31, 105-116, https://doi.org/10.11898/1001-7313.20200110, 2020.

Kong, L., Feng, M., Liu, Y., Zhang, Y., Zhang, C., Li, C., Qu, Y., An, J., Liu, X., Tan, Q., Cheng, N., Deng, Y., Zhai, R., and Wang, Z.: Elucidating the pollution characteristics of nitrate, sulfate and ammonium in PM_{2.5} in Chengdu, southwest China, based on 3-year measurements, Atmospheric Chemistry and Physics, 20, 11181-11199, https://doi.org/10.5194/acp-20-11181-2020, 2020.

Kotarba, A. Z.: Calibration of global MODIS cloud amount using CALIOP cloud profiles, Atmospheric Measurement Techniques, 13, 4995-5012, https://doi.org/10.5194/amt-13-4995-2020, 2020.

Leighton, H. G. and Ivanova, I. T.: Aerosol–Cloud Interactions in a Mesoscale Model. Part I: Sensitivity to Activation and Collision–Coalescence, Journal of the Atmospheric Sciences, 65, 289-308, https://doi.org/10.1175/2007jas2207.1, 2008.

Lelieveld, J. and Heintzenberg, J.: Sulfate cooling effect on climate through in-cloud oxidation of anthropogenic SO2, 258, 117-120, Science, https://doi.org/10.1126/science.258.5079.117, 1992.

Li, J.: Microphysical Characteristics and S(IV) Multiphase Chemical Reaction Mechanism of Orographic Clouds, Ph.D. thesis, Department of Environmental Science & Engineering, Fudan University, 113 pp., 2020.

Li, J., Zhu, C., Chen, H., Fu, H., Xiao, H., Wang, X., Herrmann, H., and Chen, J.: A More Important Role for the Ozone-S(IV) Oxidation Pathway Due to Decreasing Acidity in Clouds, Journal of Geophysical Research: Atmospheres, 125, e2020JD033220, https://doi.org/10.1029/2020jd033220, 2020a.

Li, J., Wang, X., Chen, J., Zhu, C., Li, W., Li, C., Liu, L., Xu, C., Wen, L., Xue, L., Wang, W., Ding, A., and Herrmann, H.: Chemical composition and droplet size distribution of cloud at the summit of Mount Tai, China, Atmospheric Chemistry and Physics, 17, 9885-9896, https://doi.org/10.5194/acp-17-9885-2017, 2017a.

Li, J., Zhu, C., Chen, H., Zhao, D., Xue, L., Wang, X., Li, H., Liu, P., Liu, J., Zhang, C., Mu, Y., Zhang, W., Zhang, L., Herrmann, H., Li, K., Liu, M., and Chen, J.: The evolution of cloud and aerosol microphysics at the summit of Mt. Tai, China, Atmospheric Chemistry and Physics, 20, 13735-13751, https://doi.org/10.5194/acp-20-13735-2020, 2020b.

Li, M., Liu, H., Geng, G., Hong, C., Liu, F., Song, Y., Tong, D., Zheng, B., Cui, H., Man, H., Zhang, Q., and He, K.: Anthropogenic emission inventories in China: a review, National Science Review, 4, 834-866, https://doi.org/10.1093/nsr/nwx150, 2017b.

Li, P.: Fog Water Chemistry and Fog-Haze Transformation in Shanghai, Ph.D. thesis, Department of Environmental Science & Engineering, Fudan University, 133 pp., 2011.

Liu, S. C., McKeen, S. A., Hsie, E. Y., Lin, X., Kelly, K. K., Bradshaw, J. D., Sandholm, S. T., Browell, E. V., Gregory, G. L., Sachse, G. W., Bandy, A. R., Thornton, D. C., Blake, D. R., Rowland, F. S.,

Newell, R., Heikes, B. G., Singh, H., and Talbot, R. W.: Model study of tropospheric trace species distributions during PEM-WEST A, J. Geophys. Res, 101 2073-2085, https://doi.org/10.1029/95JD02277, 1996.

Liu, T., Chan, A. W. H., and Abbatt, J. P. D.: Multiphase Oxidation of Sulfur Dioxide in Aerosol Particles: Implications for Sulfate Formation in Polluted Environments, Environ Sci Technol, 55, 4227-4242, https://doi.org/10.1021/acs.est.0c06496, 2021.

Lu, X., Zhang, S., Xing, J., Wang, Y., Chen, W., Ding, D., Wu, Y., Wang, S., Duan, L., and Hao, J.: Progress of Air Pollution Control in China and Its Challenges and Opportunities in the Ecological Civilization Era, Engineering, 6, 1423-1431, https://doi.org/10.1016/j.eng.2020.03.014, 2020.

Maahs, H. G.: Kinetics and Mechanism of the Oxidation of S(IV) by Ozone in Aqueous Solution With Particular Reference to SO2 Conversion in Nonurban Tropospheric Clouds, journal of geophysical research oceans, 88, 10721-10732, https://doi.org/10.1029/JC088iC15p10721, 1983.

Martin, G. M., Johnson D. W., and Spice A., The measurement and parameterization of effective radius in warm stratocumulus cloud, J. Atmos. Sci., 51, 1823-1842, https://doi.org/10.1175/1520-0469(1994)051<1823:TMAPOE>2.0.CO;2, 1994.

Martin, L. R. and Good, T. W.: Catalyzed oxidation of sulfur dioxide in solution: The iron-manganese synergism, Atmospheric Environment, 25, 2395-2399, https://doi.org/10.1016/0960-1686(91)90113-L, 1991.

Menut, L., Bessagnet, B., Khvorostyanov, D., Beekmann, M., Colette, A., Coll, I., Curci, G., Foret, G., Hodzic, A., Mailler, S., Meleux, F., Monge, J. L., Pison, I., Turquety, S., Valari, M., Vautard, R., and Vivanco, M. G.: Regional atmospheric composition modeling with CHIMERE, Geoscientific Model Development, 6, 981-1028, https://doi.org/10.5194/gmdd-6-203-2013, 2013.

Moch, J. M., Dovrou, E., Mickley, L. J., Keutsch, F. N., Cheng, Y., Jacob, D. J., Jiang, J., Li, M., Munger, J. W., Qiao, X., and Zhang, Q.: Contribution of Hydroxymethane Sulfonate to Ambient Particulate

Matter: A Potential Explanation for High Particulate Sulfur During Severe Winter Haze in Beijing, Geophysical Research Letters, 45, 11969-11979, https://doi.org/10.1029/2018gl079309, 2018.

Molina: Air Quality in the Mexico Megacity: An Integrated Assessment, Alliance for Global Sustainability Bookseries, 2, 141-145, https://doi.org/10.1007/978-94-010-0454-1, 2002.

Park, R. J. and Jacob, D. J.: Sources of carbonaceous aerosols over the United States and implications for natural visibility, Journal of Geophysical Research, 108, 4355, https://doi.org/10.1029/2002jd003190, 2003.

Peng, J., Hu, M., Shang, D., Wu, Z., Du, Z., Tan, T., Wang, Y., Zhang, F., and Zhang, R.: Explosive Secondary Aerosol Formation during Severe Haze in the North China Plain, Environ Sci Technol, 55, 2189-2207, https://doi.org/10.1021/acs.est.0c07204, 2021.

Pye, H. O. T., Nenes, A., Alexander, B., Ault, A. P., Barth, M. C., Clegg, S. L., Jr., J. L. C., Fahey, K. M., Hennigan, C. J., Herrmann, H., Kanakidou, M., Kelly, J. T., Ku, I.-T., McNeill, V. F., Riemer, N., Schaefer, T., Shi, G., Tilgner, A., Walker, J. T., Wang, T., Weber, R., Xing, J., Zaveri, R. A., and Zuend, a. A.: Havala O. T. Pye The acidity of atmospheric particles and clouds, Atmospheric Chemistry Physics, 20, 4809-4888, https://doi.org/10.5194/acp-20-4809-2020, 2020.

Ramanathan, V., Crutzen, P. J., Kiehl, J. T., and Rosenfeld, D.: Aerosols, climate, and the hydrological cycle, Science, 294, 2119-2124, 10.1126/science.1064034, 2001.

Ravishankara, A. R.: Heterogeneous and Multiphase Chemistry in the Troposphere, Science, 276, 1058-1065, https://doi.org/10.1126/science.276.5315.1058, 1997.

Ren, Y., Ding, A., Wang, T., Shen, X., Guo, J., Zhang, J., Wang, Y., Xu, P., Wang, X., and Gao, J.: Measurement of gas-phase total peroxides at the summit of Mount Tai in China, Atmospheric Environment, 43, 1702-1711, https://doi.org/10.1016/j.atmosenv.2008.12.020, 2009.

Sha, T., Ma, X., Jia, H., Tian, R., Chang, Y., Cao, F., and Zhang, Y.: Aerosol chemical component:

Simulations with WRF-Chem and comparison with observations in Nanjing, Atmospheric Environment, 218, 116982, https://doi.org/10.1016/j.atmosenv.2019.116982, 2019a.

Sha, T., Ma, X., Jia, H., van der A, R. J., Ding, J., Zhang, Y., and Chang, Y.: Exploring the influence of two inventories on simulated air pollutants during winter over the Yangtze River Delta, Atmospheric Environment, 206, 170-182, https://doi.org/10.1016/j.atmosenv.2019.03.006, 2019b.

Shen, X., Lee, T., Guo, J., Wang, X., Li, P., Xu, P., Wang, Y., Ren, Y., Wang, W., Wang, T., Li, Y., Carn, S. A., and Collett, J. L.: Aqueous phase sulfate production in clouds in eastern China, Atmospheric Environment, 62, 502-511, https://doi.org/10.1016/j.atmosenv.2012.07.079, 2012.

Sielski, J., Kazirod-Wolski, K., Jozwiak, M. A., and Jozwiak, M.: The influence of air pollution by PM2.5, PM10 and associated heavy metals on the parameters of out-of-hospital cardiac arrest, Sci Total Environ, 788, 147541, https://doi.org/10.1016/j.scitotenv.2021.147541, 2021.

Song, S., Gao, M., Xu, W., Sun, Y., Worsnop, D. R., Jayne, J. T., Zhang, Y., Zhu, L., Li, M., Zhou, Z., Cheng, C., Lv, Y., Wang, Y., Peng, W., Xu, X., Lin, N., Wang, Y., Wang, S., Munger, J. W., Jacob, D. J., and McElroy, M. B.: Possible heterogeneous chemistry of hydroxymethanesulfonate (HMS) in northern China winter haze, Atmospheric Chemistry and Physics, 19, 1357-1371, htttps://doi.org/10.5194/acp-19-1357-2019, 2019.

Sun, K., Liu, H., Ding, A., and Wang, X.: WRF-Chem Simulation of a Severe Haze Episode in the Yangtze River Delta, China, Aerosol and Air Quality Research, 16, 1268-1283, https://doi.org/10.4209/aaqr.2015.04.0248, 2016.

Terrenoire, E., Bessagnet, B., Rouïl, L., Tognet, F., Pirovano, G., Létinois, L., Beauchamp, M., Colette, A., Thunis, P., Amann, M., and Menut, L.: High-resolution air quality simulation over Europe with the chemistry transport model CHIMERE, Geoscientific Model Development, 8, 21-42, https://doi.org/10.5194/gmd-8-21-2015, 2015.

Tie, X.: Assessment of the global impact of aerosols on tropospheric oxidants, Journal of Geophysical

Research, 110, D03204, https://doi.org/10.1029/2004jd005359, 2005.

Tuccella, P., Curci, G., Visconti, G., Bessagnet, B., Menut, L., and Park, R. J.: Modeling of gas and aerosol with WRF/Chem over Europe: Evaluation and sensitivity study, Journal of Geophysical Research, 117, D03303, https://doi.org/10.1029/2011JD016302, 2012.

Turnock, S. T., Mann, G. W., Woodhouse, M. T., Dalvi, M., O'Connor, F. M., Carslaw, K. S., and Sprackle, D. V.: The Impact of Changes in Cloud Water pH on Aerosol, Geophysical Research Letters, 46, 4039-4048, 10.1029/2019GL082067, 2019.

Twomey: Aerosols, clouds and radiation, Atmospheric Environment.part A.general Topics, 25, 2435-2442, https://doi.org/10.1016/0960-1686(91)90159-5, 1991.

Twomey, S. A., Piepgrass, M., and Wolfe, T. L.: An assessment of the impact of pollution on the global cloud albedo, Tellus B: Chemical and Physical Meteorology, 36B, 356-366, https://doi.org/10.1111/j.1600-0889.1984.tb00254.x, 1984.

von Salzen, K., Leighton, H. G., Ariya, P. A., Barrie, L. A., Gong, S. L., Blanchet, J. P., Spacek, L., Lohmann, U., and Kleinman, L. I.: Sensitivity of sulphate aerosol size distributions and CCN concentrations over North America to SOx emissions and H2O2 concentrations, Journal of Geophysical Research: Atmospheres, 105, 9741-9765, https://doi.org/10.1029/2000jd900027, 2000.

Wang, G., Zhang, R., Gomez, M. E., Yang, L., Levy Zamora, M., Hu, M., Lin, Y., Peng, J., Guo, S., Meng, J., Li, J., Cheng, C., Hu, T., Ren, Y., Wang, Y., Gao, J., Cao, J., An, Z., Zhou, W., Li, G., Wang, J., Tian, P., Marrero-Ortiz, W., Secrest, J., Du, Z., Zheng, J., Shang, D., Zeng, L., Shao, M., Wang, W., Huang, Y., Wang, Y., Zhu, Y., Li, Y., Hu, J., Pan, B., Cai, L., Cheng, Y., Ji, Y., Zhang, F., Rosenfeld, D., Liss, P. S., Duce, R. A., Kolb, C. E., and Molina, M. J.: Persistent sulfate formation from London Fog to Chinese haze, Proc Natl Acad Sci U S A, 113, 13630-13635, https://doi.org/10.1073/pnas.1616540113, 2016.

Wang, H., Shi, G. Y., Zhang, X. Y., Gong, S. L., Tan, S. C., Chen, B., Che, H. Z., and Li, T.: Mesoscale

modelling study of the interactions between aerosols and PBL meteorology during a haze episode in China Jing–Jin–Ji and its near surrounding region – Part 2: Aerosols' radiative feedback effects, Atmospheric Chemistry and Physics,15,6(2015-03-23), 14, 3277-3287, https://doi.org/10.5194/acp-15-3257-2015, 2015.

Wang, J., Li, J., Ye, J., Zhao, J., Wu, Y., Hu, J., Liu, D., Nie, D., Shen, F., Huang, X., Huang, D. D., Ji, D., Sun, X., Xu, W., Guo, J., Song, S., Qin, Y., Liu, P., Turner, J. R., Lee, H. C., Hwang, S., Liao, H., Martin, S. T., Zhang, Q., Chen, M., Sun, Y., Ge, X., and Jacob, D. J.: Fast sulfate formation from oxidation of SO2 by NO2 and HONO observed in Beijing haze, Nature Communications, 11, 2844, https://doi.org/10.1038/s41467-020-16683-x, 2020.

Wang, S., Zhou, S., Tao, Y., Tsui, W. G., Ye, J., Yu, J. Z., Murphy, J. G., McNeill, V. F., Abbatt, J. P. D., and Chan, A. W. H.: Organic Peroxides and Sulfur Dioxide in Aerosol: Source of Particulate Sulfate, Environ Sci Technol, 53, 10695-10704, https://doi.org/10.1021/acs.est.9b02591, 2019.

Wang, T., Liu, M., Liu, M., Song, Y., Xu, Z., Shang, F., Huang, X., Liao, W., Wang, W., Ge, M., Cao, J., Hu, J., Tang, G., Pan, Y., Hu, M., and Zhu, T.: Sulfate Formation Apportionment during Winter Haze Events in North China, Environ Sci Technol, 56, 7771-7778, https://doi.org/10.1021/acs.est.2c02533, 2022.

Wang, W., Liu, M., Wang, T., Song, Y., Zhou, L., Cao, J., Hu, J., Tang, G., Chen, Z., Li, Z., Xu, Z., Peng, C., Lian, C., Chen, Y., Pan, Y., Zhang, Y., Sun, Y., Li, W., Zhu, T., Tian, H., and Ge, M.: Sulfate formation is dominated by manganese-catalyzed oxidation of SO(2) on aerosol surfaces during haze events, Nat Commun, 12, 1993, https://doi.org/10.1038/s41467-021-22091-6, 2021.

Wang, Y., Zhang, Q. Q., Jiang, J., Zhou, W., Wang, B., He, K., Duan, F., Zhang, Q., Philip, S., and Xie, Y.: Enhanced sulfate formation during China's severe winter haze episode in January 2013 missing from current models, Journal of Geophysical Research Atmospheres, 119, 10425-10440, https://doi.org/10.1002/2013JD021426, 2014.

Wei, Y., Chen, X., Chen, H., Li, J., Wang, Z., Yang, W., Ge, B., Du, H., Hao, J., Wang, W., Li, J., Sun, Y.,

and Huang, H.: IAP-AACM v1.0: a global to regional evaluation of the atmospheric chemistry model in CAS-ESM, Atmospheric Chemistry and Physics, 19, 8269-8296, https://doi.org/10.5194/acp-19-8269-2019, 2019.

Xie, Y., Dai, H., Zhang, Y., Wu, Y., Hanaoka, T., and Masui, T.: Comparison of health and economic impacts of PM2.5 and ozone pollution in China, Environ Int, 130, 104881, https://doi.org/10.1016/j.envint.2019.05.075, 2019.

Yao, M., Zhao, Y., Hu, M., Huang, D., Wang, Y., Yu, J. Z., and Yan, N.: Multiphase Reactions between Secondary Organic Aerosol and Sulfur Dioxide: Kinetics and Contributions to Sulfate Formation and Aerosol Aging, Environmental Science & Technology Letters, 6, 768-774, htttps://doi.org/10.1021/acs.estlett.9b00657, 2019.

Yao, S., Wang, Q., Zhang, J., and Zhang, R.: Characteristics of Aerosol and Effect of Aerosol-Radiation-Feedback in Handan, an Industrialized and Polluted City in China in Haze Episodes, Atmosphere, 12, 670, https://doi.org/10.3390/atmos12060670, 2021.

Ye, C., Xue, C., Zhang, C., Ma, Z., Liu, P., Zhang, Y., Liu, C., Zhao, X., Zhang, W., He, X., Song, Y., Liu, J., Wang, W., Sui, B., Cui, R., Yang, X., Mei, R., Chen, J., and Mu, Y.: Atmospheric Hydrogen Peroxide H2O2 at the Foot and Summit of Mt Tai Variations Sources, Journal of Geophysical Research: Atmospheres, 126, e2020JD033975, https://doi.org/10.1029/2020JD033975, 2021.

Ye, J., Abbatt, J. P. D., and Chan, A. W. H.: Novel pathway of SO2 oxidation in the atmosphere: reactions with monoterpene ozonolysis intermediates and secondary organic aerosol, Atmospheric Chemistry and Physics, 18, 5549-5565, htttps://doi.org/10.5194/acp-18-5549-2018, 2018.

Zhang, L., Gong, S., Zhao, T. L., Zhou, C. H., and Zhang, X. Y.: Development of WRF/CUACE v1.0 model and its preliminary application in simulating air quality in China, Geoscientific Model Development, 14, 703-718, https://doi.org/10.5194/gmd-14-703-2021, 2021.

Zhang, X. Y., Wang, Y. Q., Niu, T., Zhang, X. C., Gong, S. L., Zhang, Y. M., and Sun, J. Y.: Atmospheric

aerosol compositions in China: spatial/temporal variability, chemical signature, regional haze distribution and comparisons with global aerosols, Atmospheric Chemistry and Physics, 12, 779-799, https://doi.org/10.5194/acp-12-779-2012, 2012.

Zheng, B., Tong, D., Li, M., Liu, F., Hong, C., Geng, G., Li, H., Li, X., Peng, L., Qi, J., Yan, L., Zhang, Y., Zhao, H., Zheng, Y., He, K., and Zhang, Q.: Trends in China's anthropogenic emissions since 2010 as the consequence of clean air actions, Atmospheric Chemistry and Physics, 18, 14095-14111, https://doi.org/10.5194/acp-18-14095-2018, 2018.

Zhou, C., Zhang, X., Zhang, J., and Zhang, X.: Representations of dynamics size distributions of mineral dust over East Asia by a regional sand and dust storm model, Atmospheric Research, 250, 18965, https://doi.org/10.1016/j.atmosres.2020.105403, 2021a.

Zhou, C. H., Zhang, X. Y., Gong, S., Wang, Y. Q., and Xue, M.: Improving aerosol interaction with clouds and precipitation in a regional chemical weather modeling system, Atmospheric Chemistry and Physics, 16, 145-160, https://doi.org/10.5194/acp-16-145-2016, 2016.

Zhou, C. H., Gong, S., Zhang, X. Y., Liu, H. L., Xue, M., Cao, G. L., An, X. Q., and Che, H. Z.: Towards the improvements of simulating the chemical and optical properties of Chinese aerosols using an online coupled model - CUACE/Aero, Tellus B: Chemical and Physical Meteorology, 64, https://doi.org/10.3402/tellusb.v64i0.18965, 2012.

Zhou, Y., Gong, S., Zhou, C., Zhang, L., He, J., Wang, Y., Ji, D., Feng, J., Mo, J., and Ke, H.: A new parameterization of uptake coefficients for heterogeneous reactions on multi-component atmospheric aerosols, Sci Total Environ, 781, 146372, https://doi.org/10.1016/j.scitotenv.2021.146372, 2021b.

Zhu, Y., Yang, L., Chen, J., Kawamura, K., Sato, M., Tilgner, A., van Pinxteren, D., Chen, Y., Xue, L., Wang, X., Simpson, I. J., Herrmann, H., Blake, D. R., and Wang, W.: Molecular distributions of dicarboxylic acids, oxocarboxylic acids and α-dicarbonyls in PM2.5 collected at the top of Mt. Tai, North China, during the wheat burning season of 2014, Atmospheric Chemistry and Physics, 18, 10741-10758, https://doi.org/10.5194/acp-18-10741-2018, 2018.

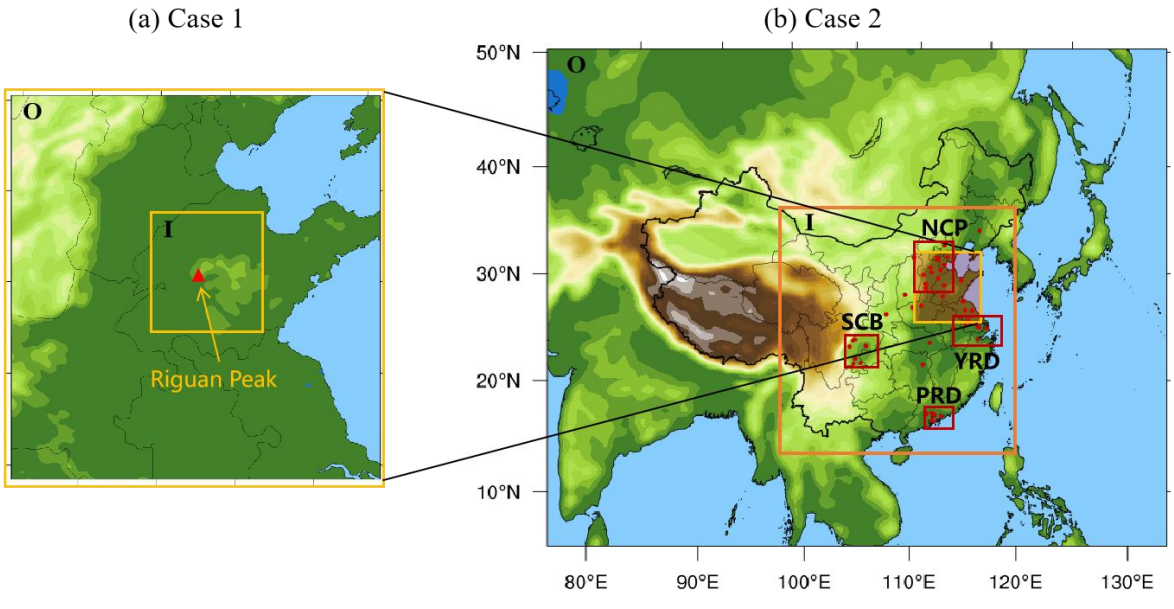

Figure 1. Model nesting domains and target regions. (a) Case 1. The red triangle is the Mount Tai observation site. (b) Case 2. Red dots are some cities where the surface observations of air pollutants are used for model evaluation. The target four regions are NCP for the North China Plain, YRD for the Yangtze River Delta, PRD for the Pearl River Delta and SCB for the Sichuan Basin.

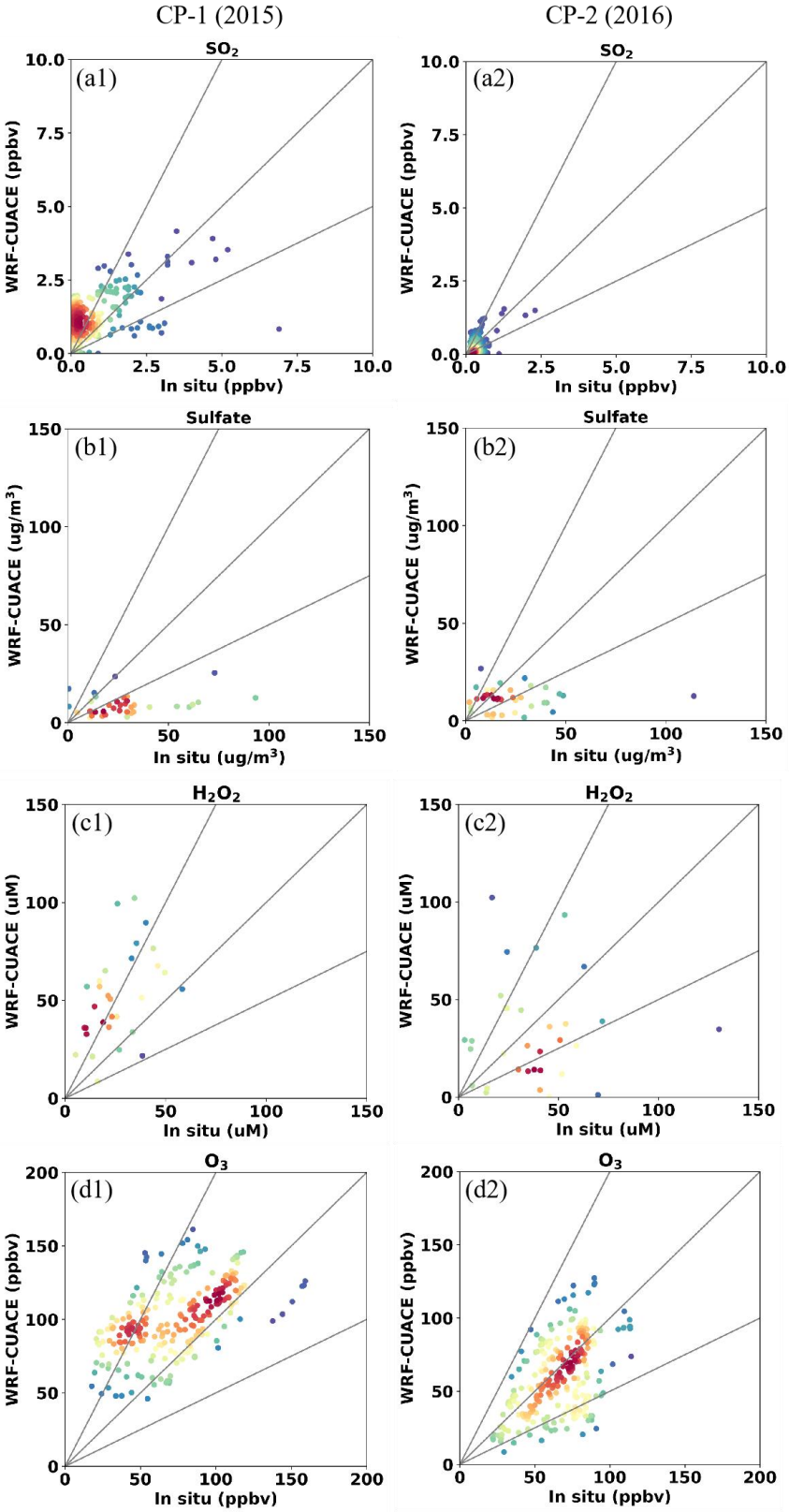

Figure 2. Scatter plots of hourly SO_2 (a1, a2), sulfate (b1, b2), H_2O_2 (c1, c2) and O_3 (d1, d2) concentrations between WRF/CUACE and in situ observations at Mount Tai in CP-1 and CP-2. Units: SO_2 and O_3 (ppbv), H_2O_2 (μM), and Sulfate (μg/m^3). The color of the dots represents the point density, and the red means more sample size.

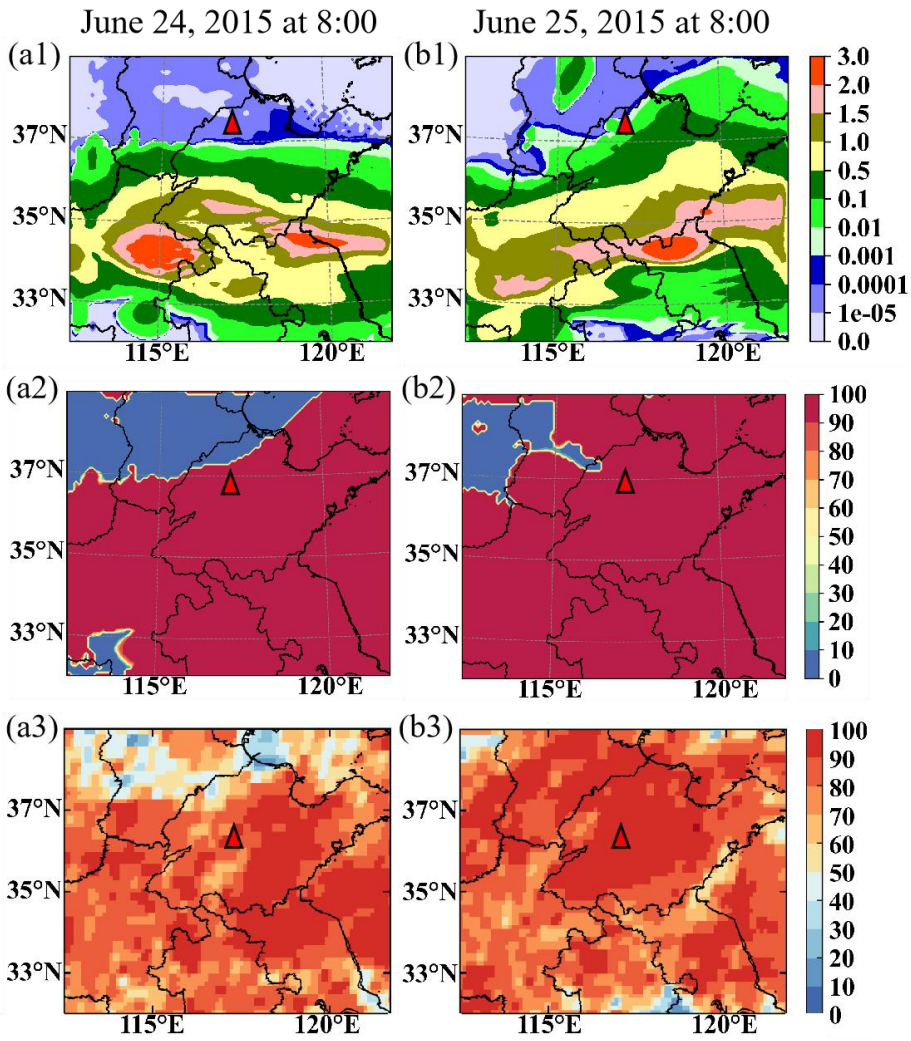

Figure 3. Cloud water simulation and satellite comparison. The column liquid water content by WRF/CUACE (a1, b1, Units: kg/m^2), the cloud fraction by WRF/CUACE.(a2, b2, Units: %) and the cloud total amount of FY2G, (a3, b3, Units: %). (a) is for 8:00 LST on 24 June 2015, (b) is for 8:00 LST on 25 June 2015. The red triangle is the Mount Tai observation site.

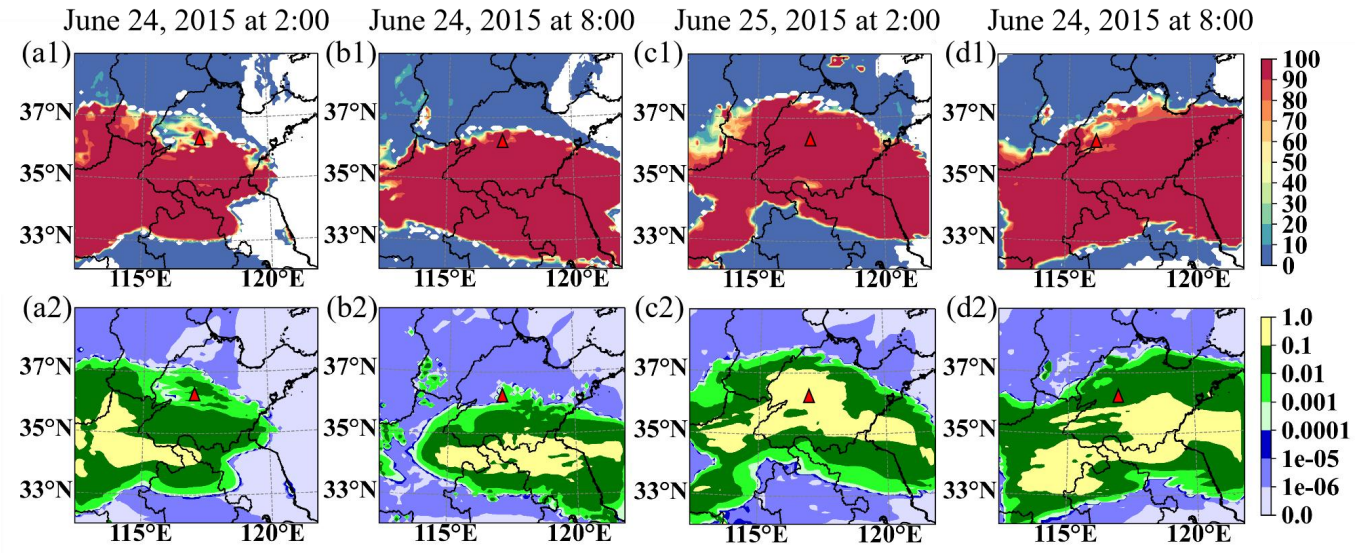

Figure 4. Regional comparison of in-cloud SO_2 oxidation with cloud water at the high of Mount Tai. Distributions of SO_2 oxidation rate (a1, b1, c1 and d1, Units: %) and the liquid water content (a2, b2, c2 and d2, Units: g/kg) by WRF/CUACE, where (a) is for 2:00 LST on 24 June 2015, (b) is for 8:00 LST on 24 June 2015, (c) is for 2:00 LST on 25 June 2015 and (d) is for 8:00 LST on 25 June 2015. The red triangle is the Mount Tai observation site.

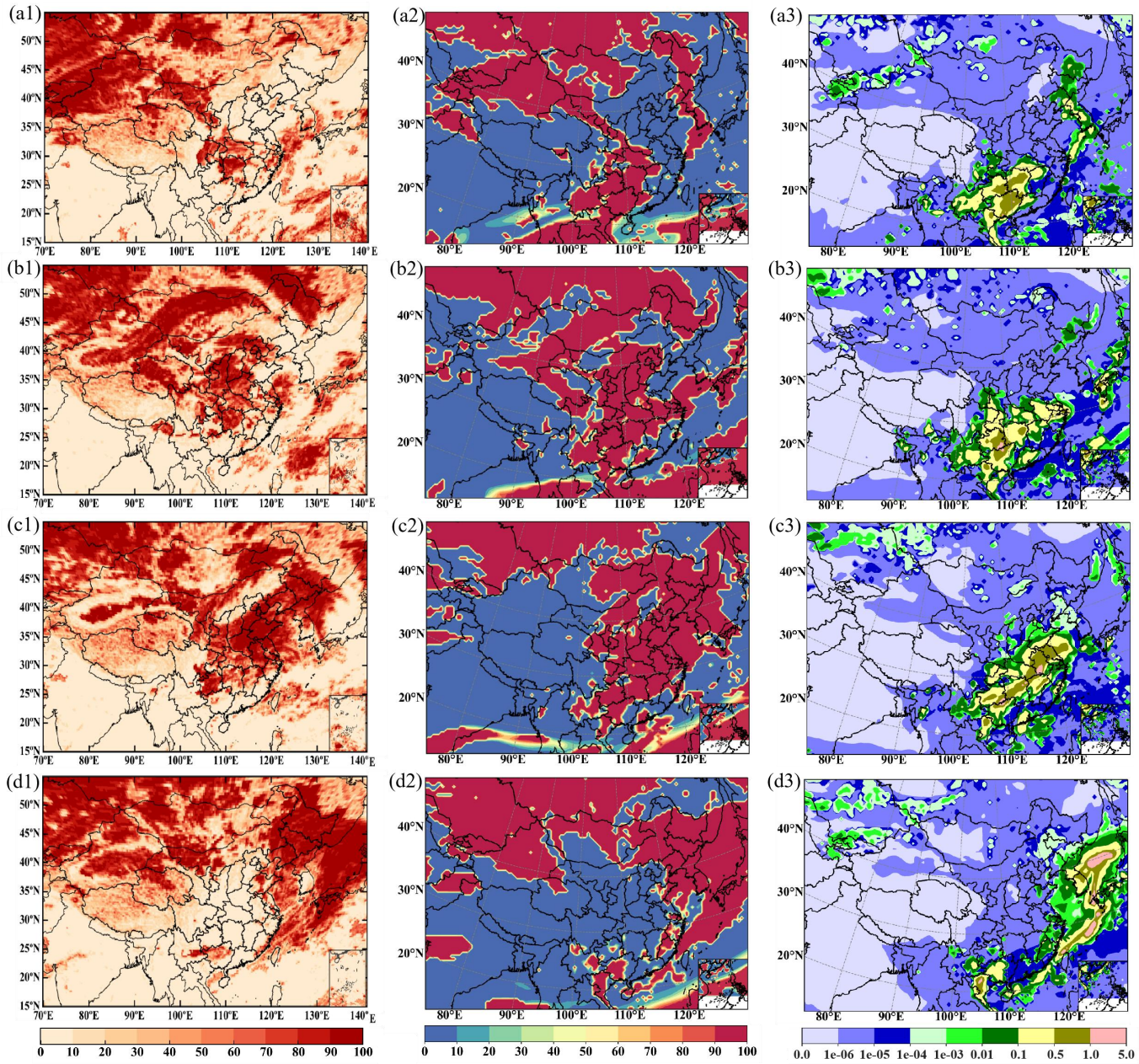

Figure 5. Cloud water simulation and satellite comparison in a heavy pollution episode. The cloud total amount of FY-2G (a1, b1, c1, d1, Units: %), the column cloud of WRF/CUACE (a2, b2, c2, d2, Units: %) and the column liquid water content of WRF/CUACE (a3, b3, c3, d3, Units: kg/m^2). (a) is for 8:00 LST on 19 Dec., (b) is for 8:00 LST on 20 Dec., (c) is for 8:00 LST on 21 Dec., and (d) is for 8:00 LST on 22 Dec.

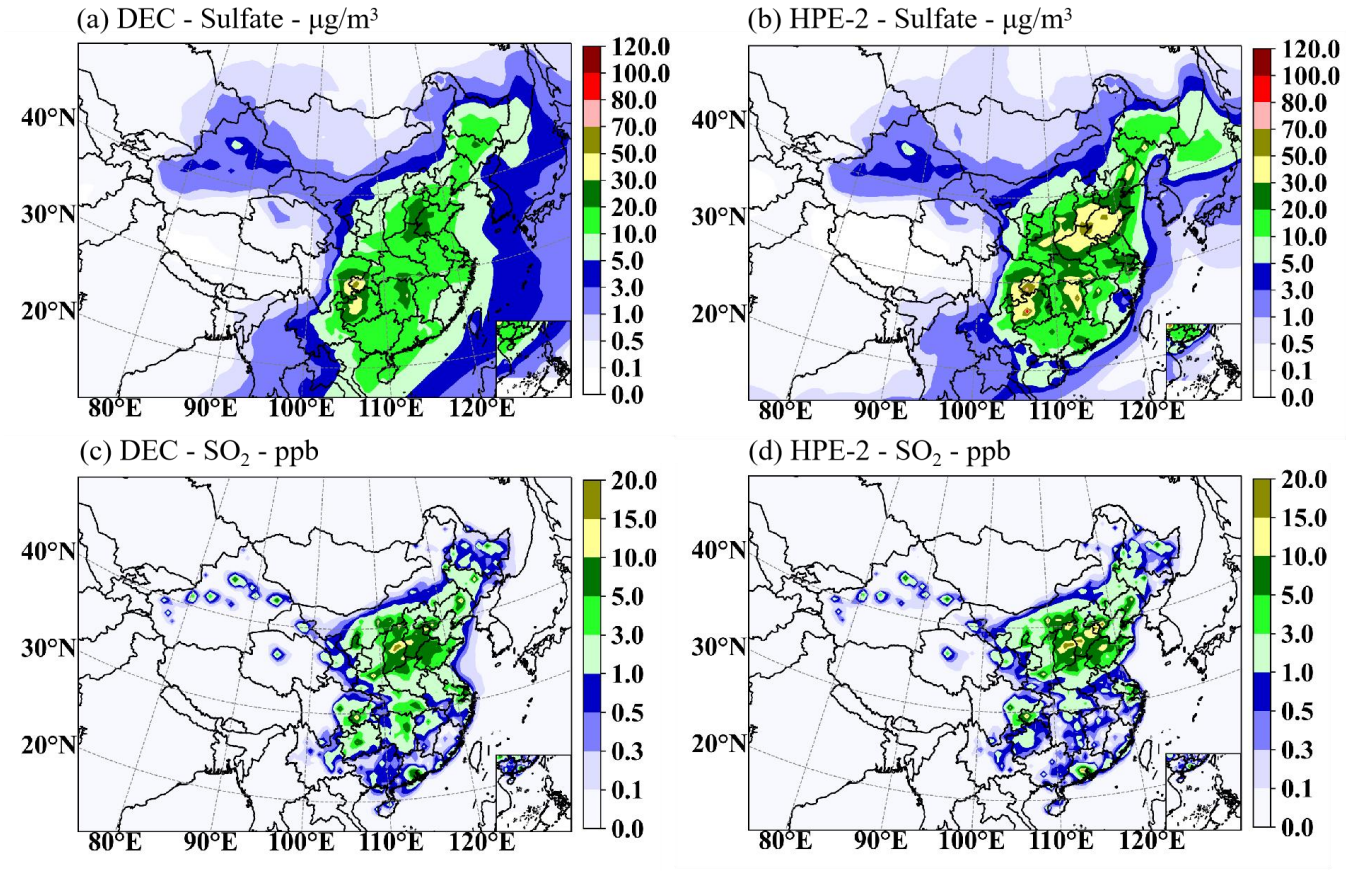

Figure 6. The mean sulfate concentration for DEC (a, c) and HPE-2 (b, d) for SO_2 (c, e) and sulfate (a, b).

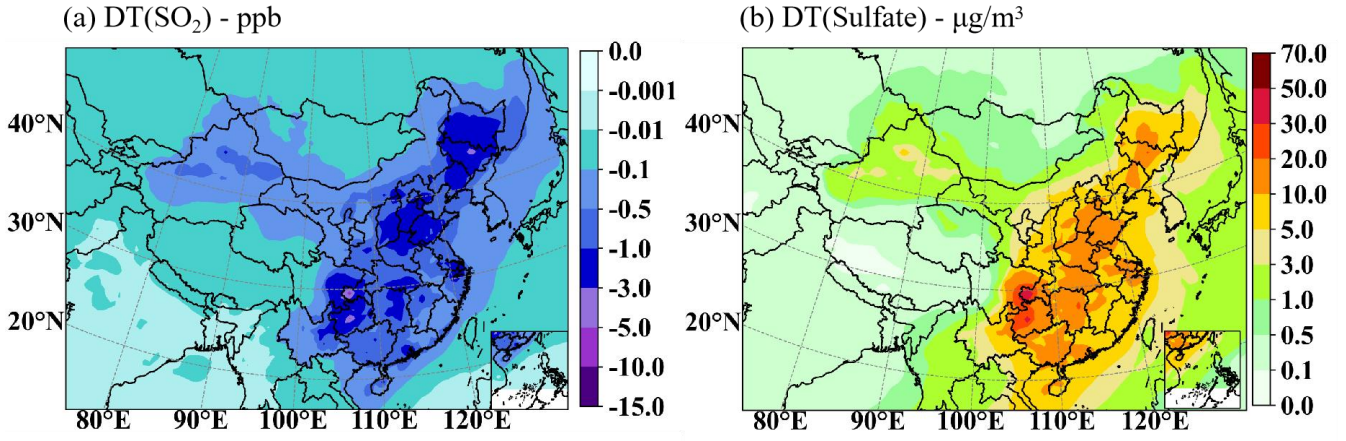

Figure 7. The mean SO_2 concentration decreased (a) and sulfate concentration increased (b) by cloud chemistry for DEC.

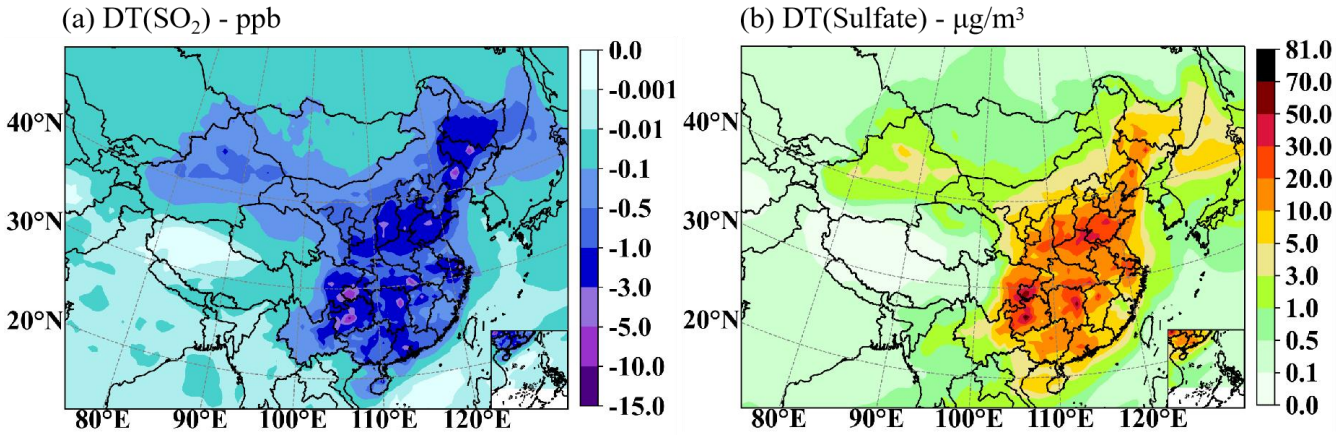

Figure 8. The mean SO_2 concentration decreased (a) and sulfate concentration increased (b) by cloud chemistry for HPE-2.

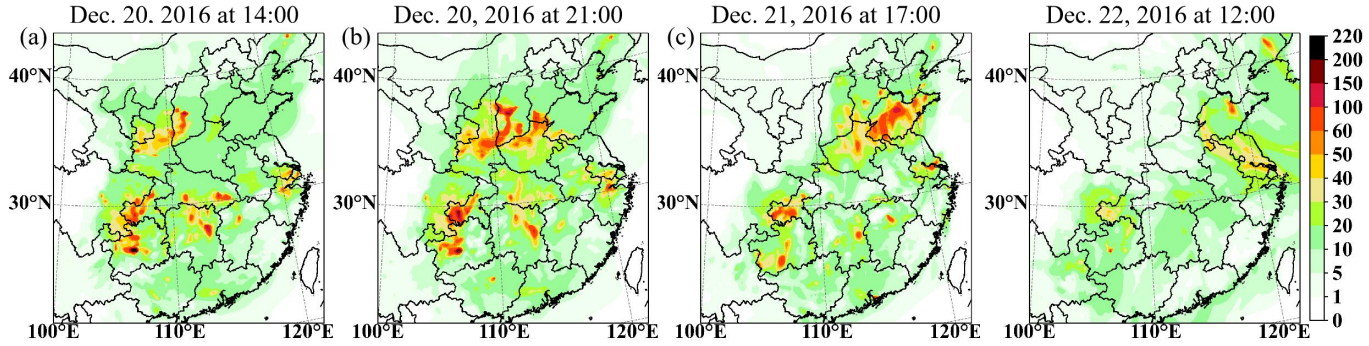

Figure 9. The differences in surface sulfate concentrations between with and without cloud chemistry at 21:00 LST on 20 Dec. (a), at 17:00 LST on 21 Dec. (b), and at 12:00 LST on 22 Dec. (c) (Units: μg/m^3).

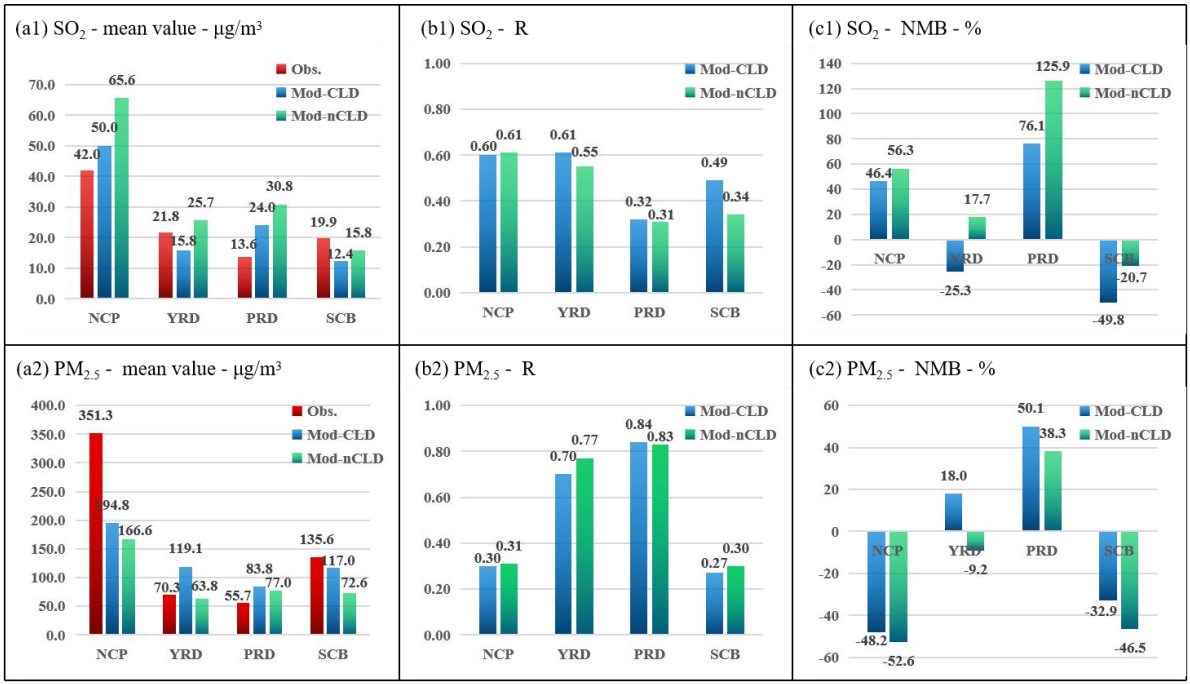

Figure 10. Statistical metrics for hourly SO_2 and $PM_{2.5}$ for four regions for HPE-2 with (Mod-CLD) and without (Mod-nCLD) cloud chemistry. The mean value (a1, Units: μg/m^3), R (b1) and NMB (c1, Units: %) of SO_2 as well as the mean value (a2, Units: μg/m^3) , R (b2) and NMB (c2, Units: %) of $PM_{2.5}$. Obs. denotes the observations.

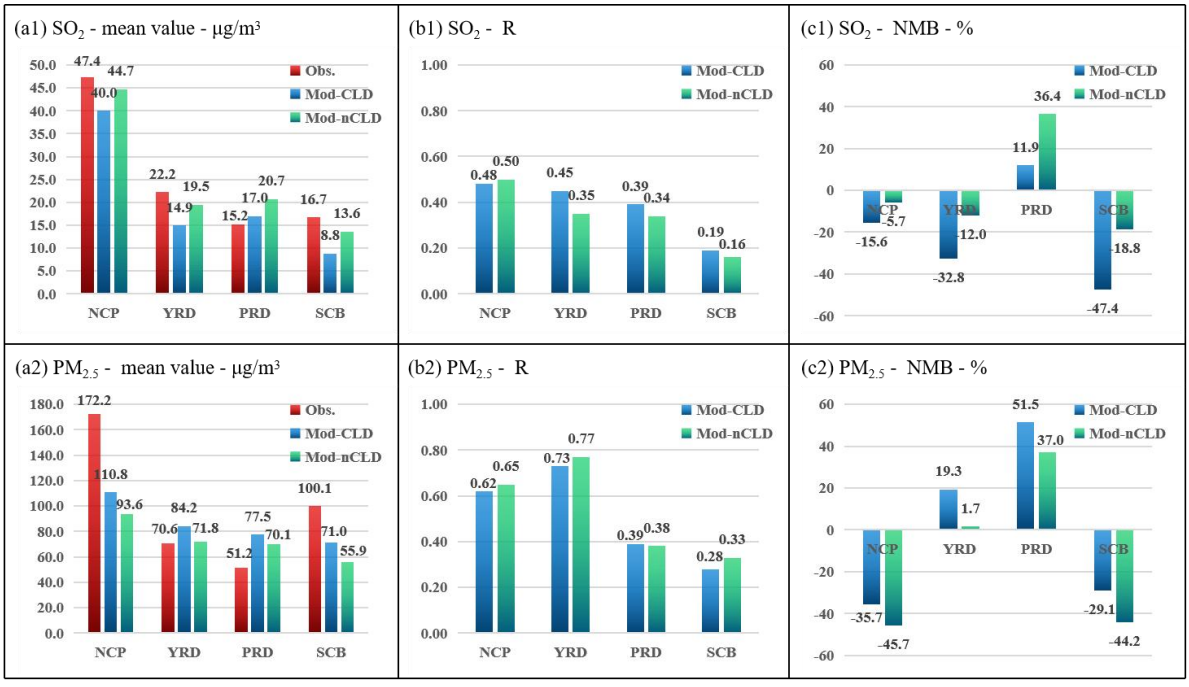

Figure 11. Statistical metrics for hourly SO_2 and $PM_{2.5}$ for four regions for DEC with (Mod-CLD) and without (Mod-nCLD) cloud chemistry. The mean value (a1, Units: μg/m^3) , R (b1) and NMB (c1, Units: %) of SO_2 as well as the mean value (a2, Units: μg/m^3) , R (b2) and NMB (c2, Units: %) of $PM_{2.5}$. Obs. denotes the observations.

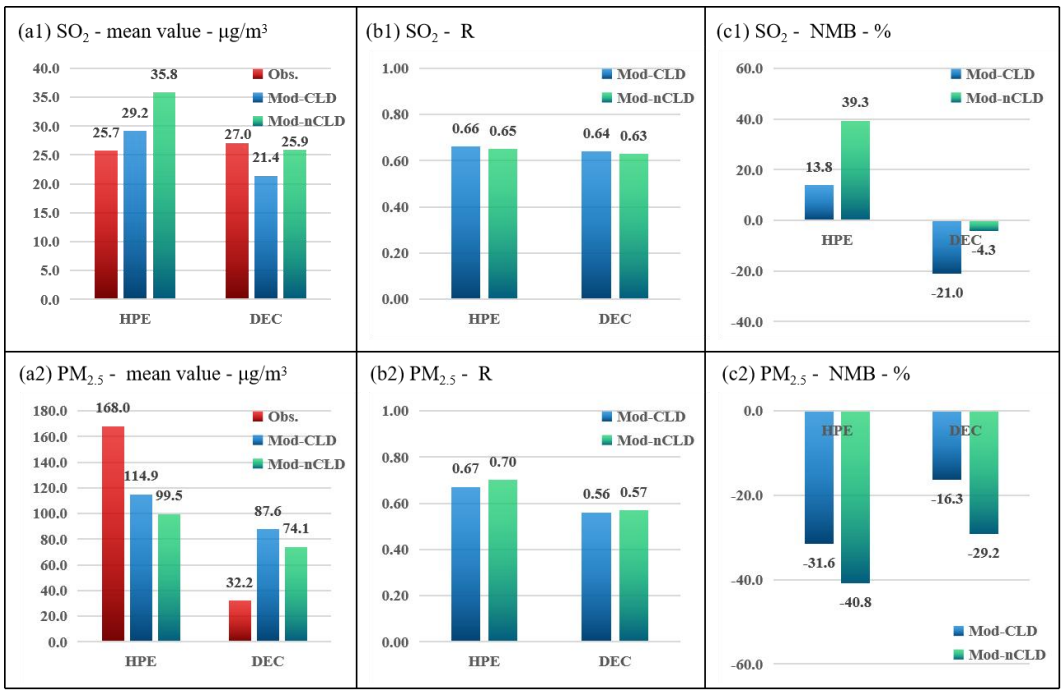

Figure 12. Statistical metrics for hourly SO_2 and $PM_{2.5}$ in all selected sites for HPE-2 and DEC with (Mod-CLD) and without (Mod-nCLD) cloud chemistry. The mean value (a1, Units: μg/m^3) , R (b1) and NMB (c1, Units: %) of SO_2 as well as the mean value (a2, Units: μg/m^3) , R (b2) and NMB (c2, Units: %) of $PM_{2.5}$. Obs. denotes the observations.

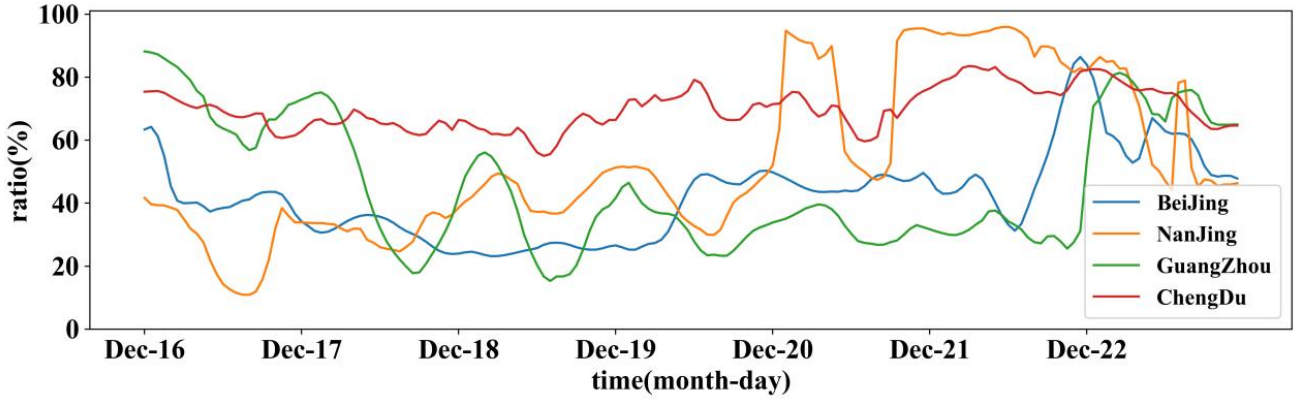

Figure 13. The rates of SO_2 column concentration reduced by cloud chemistry in Beijing (blue), Nanjing (yellow), Guangzhou (green) and Chengdu (red).

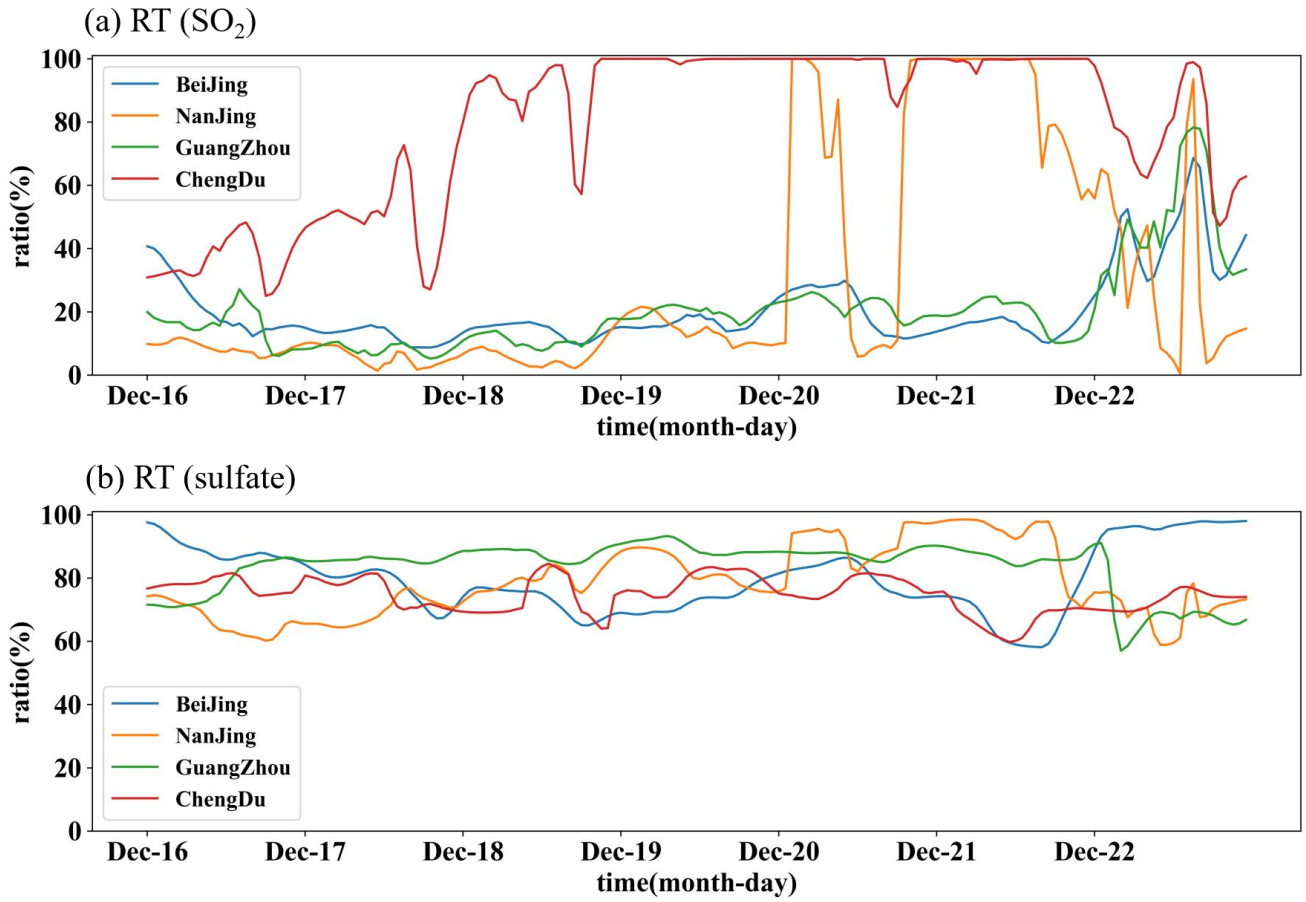

Figure 14. The rates of surface SO_2 reduced (a) and the surface sulfate increased (b) influenced by cloud chemistry in Beijing (blue), Nanjing (yellow), Guangzhou (green) and Chengdu (red).

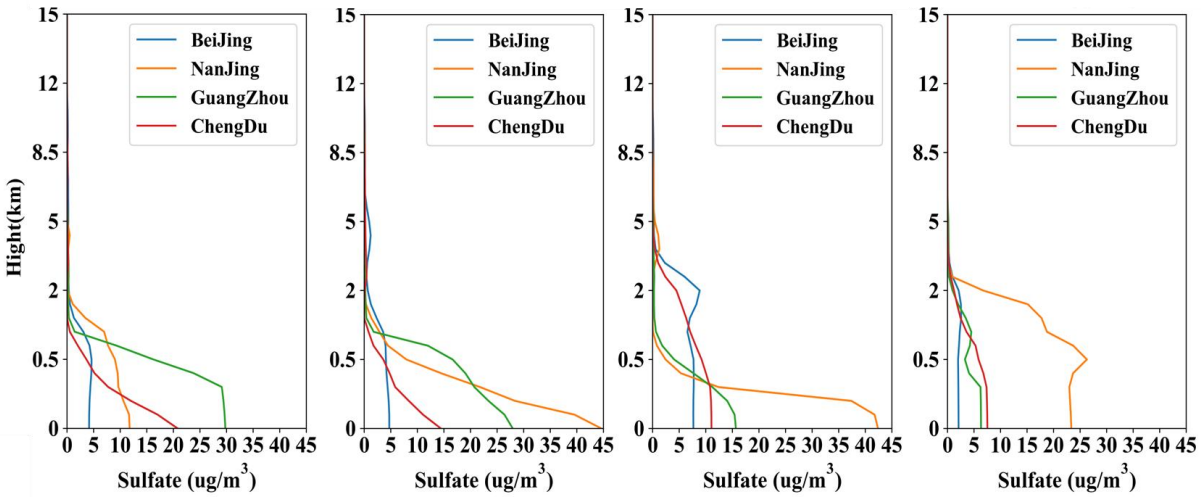

Figure 15. Vertical profiles of sulfate concentration difference (DT) at 12:00 on 20 Dec., at 21:00 on 20 Dec., at 17:00 on 21 Dec., and at 12:00 on 22 Dec. in Beijing (blue), Nanjing (yellow), Guangzhou (green) and Chengdu (red).

Table 1. Equilibrium Constants for the Parameterization of the Cloud Chemistry in CUACE.

Equilibrium Relation	Constant Expression	Equilibrium Constant		
		K(298)	a	Unit
$SO_2(g)+H_2O(aq)\leftrightarrow SO_2(aq)$	$K_{HS}=\frac{[SO_2(aq)]}{[SO_2(g)]}$	1.23	3120	$\frac{M}{\text{atm}}$
$SO_2(aq)\leftrightarrow H^+ + HSO_3^-$	$K_{1S}=\frac{[H^+][HSO_3^-]}{[SO_2(aq)]}$	1.7×10^{-2}	2090	M
$HSO_3^- \leftrightarrow H^+ + SO_3^{2-}$	$K_{2S}=\frac{[H^+][SO_3^{2-}]}{[HSO_3^-]}$	6.0×10^{-8}	1120	M
$O_3(g)+H_2O(aq)\leftrightarrow O_3(aq)$	$K_{HO}=\frac{[O_3(aq)]}{[O_3(g)]}$	1.15×10^{-2}	2560	$\frac{M}{\text{atm}}$
$H_2O_2(g)+H_2O(aq)\leftrightarrow H_2O_2(aq)$	$K_{HP}=\frac{[H_2O_2(aq)]}{[H_2O_2(g)]}$	9.7×10^{4}	6600	$\frac{M}{\text{atm}}$

Table 2. physics parameterization schemes in WRF.

Physical management	Parameterization	References
microphysics scheme	Lin	Lin et al. (1983)
shortwave radiation	Goddard	Chou and Suarez (1994)
longwave radiation	RRTM	Mlawer et al. (1997)
land surface scheme	Noah	Chen and Dudhia (2001)
boundary layer scheme	MYJ	Janjić (1994)
cumulus scheme	Grell-3D	Grell (1993)

Table 3. Statistics for SO_2, O_3, H_2O_2 and sulfate in cloud chemistry at Mount Tai site.

		Observed Mean	Simulated Mean	R	RAD (%)	NMB (%)
CP-1	SO_2	2.2	2.3	0.34	-3.4	7.1
	O_3	97.8	55.3	0.33	27.8	-43.5
	H_2O_2	26.5	16.8	0.78	22.4	-36.6
	Sulfate	31.7	9.2	0.32	55.0	-71.0
CP-2	SO_2	0.6	0.6	0.47	-6.1	12.9
	O_3	60.7	51.0	0.40	8.7	-16.0
	H_2O_2	46.9	32.4	0.06	18.4	-29.6
	Sulfate	28.1	11.4	0.54	42.2	-59.4

Note: unit of SO_2 and O_3 (ppbv), H_2O_2 (μM), and Sulfate (μg/m^3)

Table 4. Statistical metrics for meteorology in four regions for HPE and DEC

		Observed Mean		Simulated Mean		R		NMB(%)		RMSE	
		HPE	**DEC**	**HPE**	**DEC**	**HPE**	**DEC**	**HPE**	**DEC**	**HPE**	**DEC**
NCP	T2	1.0	1.1	2.8	2.1	0.70	0.84	187.3	84.9	3.3	2.5
	RH2	78.8	68.3	52.3	48.8	0.54	0.64	-33.7	-28.6	32.3	25.9
	WS10	1.5	1.7	1.7	2.2	0.49	0.54	14.1	27.5	1.2	1.3
YRD	T2	9.2	8.0	9.5	8.4	0.94	0.96	2.9	5.1	1.4	1.3
	RH2	79.2	75.6	73.8	73.0	0.86	0.85	-6.8	-3.5	10.7	9.3
	WS10	2.2	2.3	2.8	3.0	0.74	0.76	28.7	31.9	1.2	1.3
PRD	T2	18.3	17.3	19.0	17.9	0.93	0.92	3.6	3.8	1.9	1.9
	RH2	72.2	70.4	64.3	65.4	0.76	0.68	-10.9	-7.2	14.0	13.9
	WS10	1.8	2.4	2.0	3.2	0.67	0.72	13.6	37.1	1.0	1.5
SCB	T2	10.2	9.7	10.5	10.0	0.74	0.75	2.8	3.1	1.8	2.2
	RH2	81.6	79.9	74.1	71.3	0.66	0.60	-9.2	-10.8	12.7	15.5
	WS10	1.1	1.3	1.6	1.9	0.49	0.36	49.2	50.5	1.0	1.3

Note: unit of T2 (℃), RH2(%) and WS10 (m/s)

Table 5. Statistical metrics for hourly SO_2, O_3 and $PM_{2.5}$ in four regions for HPE and DEC

		Observed Mean (μg/m^3)		Simulated Mean (μg/m^3)		R		NMB(%)	
		HPE	**DEC**	**HPE**	**DEC**	**HPE**	**DEC**	**HPE**	**DEC**
NCP	SO_2	42.0	61.5	50.0	40.0	0.60	0.48	46.3	-15.6
	O_3	8.8	7.4	7.4	10.9	0.47	0.60	-15.3	-32.4
	$PM_{2.5}$	351.3	182.1	194.8	110.8	0.30	0.62	-48.2	-35.7
YRD	SO_2	21.8	16.3	15.8	14.9	0.61	0.45	-25.3	-32.8
	O_3	31.3	14.4	9.3	22.1	0.33	0.68	-54.0	-45.5
	$PM_{2.5}$	70.3	82.9	119.1	84.2	0.70	0.73	18.0	19.3
PRD	SO_2	13.6	24.0	24.0	17.0	0.32	0.39	76.1	11.9
	O_3	45.7	56.3	56.5	57.4	0.84	0.80	23.0	13.9
	$PM_{2.5}$	55.7	83.6	83.8	77.5	0.84	0.39	50.1	51.5
SCB	SO_2	20.0	10.0	12.4	8.8	0.49	0.19	-49.8	-47.4
	O_3	22.0	49.0	45.3	54.2	0.20	0.47	123.1	97.4
	$PM_{2.5}$	135.6	91.0	117.0	71.0	0.27	0.28	-32.9	-29.1